AN ASYMPTOTIC SOLUTION FOR THE DIFFRACTION BY A DIELECTRIC CYLINDER

A Thesis

Presented to

The Faculty of Graduate Studies and Research

The University of Manitoba

In Partial Fulfillment

of the Requirements for the Degree

Master of Science

in

Electrical Engineering

---

by

Wayne Sharpe Hammond

October 1966

ABSTRACT

The geometrical theory of diffraction by J.B. Keller, is used to solve for the field scattered by an infinitely long dielectric cylinder, excited by a line source parallel to the axis of the cylinder. The geometrical optics rays are used to calculate the field due to the incident, reflected and refracted rays, while the surface rays are used to determine the diffracted field at a remote observation point. It is shown that the total field predicted by this method, for cylinder diameters greater than a wavelength, is in good agreement with experiment and with the more complicated methods based on the exact solution.

ACKNOWLEDGEMENTS

The author wishes to acknowledge the assistance given by Professor M.A.K. Hamid who suggested the problem and supervised the work throughout.

Sincere thanks are also due to Professor H.R. Coish of the Department of Mathematical Physics for many hours of profitable discussion. The author expresses his appreciation to Mrs. C. LeBlanc for the excellent typing of the manuscript.

The financial assistance of the National Research Council of Canada in the form of Grant A-3326 is also acknowledged.

DEDICATION

This thesis is dedicated to my Wife,

VIVI

without whose infinite patience and understanding, it never would have been possible.

TABLE OF CONTENTS

TABLE OF CONTENTS (Continued...)

LIST OF FIGURES

INTRODUCTION

The study of scattering from dielectric objects has been stimulated by new methods of radar meteorology, and investigations of plasma columns which can be simulated by dielectric cylinders with the relative permittivity less than unity. Furthermore, this investigation is important in that, it may lead to simple solutions for the dielectric wedge or more complicated dielectric bodies (grain insects, cancer tumors, etc.) which may be approximated by cylindrical or spherical shapes.

A reliable method for predicting the field scattered by a dielectric cylinder, is naturally of interest to those engaged in the design or application of dielectric antennas or dielectric discontinuities in waveguide structures.

The problem of scattering by a dielectric cylinder was studied in a classical sense by Rayleigh(19), while an exact solution was obtained by Wait(17) and Streifer and Kodis(12). The exact solution, however, presents serious computational difficulties. A simple solution was attempted by Kouyoumjian(9) using the geometrical optics rays to determine the back-scattering radar cross-section of the cylinder. Thus only the "glory" ray and the "rainbow" ray were considered and the results are applicable only in the region of the back-scatter.

The purpose of this thesis is to apply the geometrical theory of diffraction to the problem of a dielectric cylinder in order to predict the field at any location of the observation point due to all incident, reflected, transmitted and diffracted rays passing through that point. The concept of the field on a ray is then used to derive simple expressions for the field due to the various types of rays and the desired field is finally obtained as the vector sum. The analysis is restricted to an infinitely long cylinder excited by a line source parallel to the axis of the cylinder. Furthermore, the distance to the source and the distance to the observation point are assumed to be much greater than one wavelength at the frequency of operation and the diameter of the cylinder is greater than a wavelength. These restrictions may, however, be removed by considering the next higher order terms in the asymptotic series solution.

The method is finally established theoretically, by an agreement with the leading terms of the asymptotic expansion of the exact solution for the case of the TM mode, and the diffraction coefficients are determined by comparison with this solution. The method is also in agreement with the results of Kodis[18].

The Steady State solution does not take into account the time dependence, $e^{j\omega t}$.

CHAPTER I

THE GEOMETRICAL THEORY OF DIFFRACTION

1.1 Basic Concepts of the Ray Method

The geometrical theory of diffraction as given by Keller[1,2] is based on Maxwell's Equations. It employs ray tracing diagrams as a means of obtaining asymptotic or approximate solutions to field problems. According to the theory, fields travel along certain curves, called rays, determined by the laws of geometrical optics and Fermat's principle. The total field is composed of the field on the incident and reflected optical rays plus the field due to the diffracted rays. Diffracted rays are produced by incident rays which hit edges or corners of boundary surfaces leading to edge rays emanating in all directions.

The field at an observation point is the sum of the fields on all the rays passing through that point. In general, the field on each ray consists of an amplitude term and a phase term. The amplitude term is dependent on whether the source of the ray is a spherical, cylindrical or a plane wave. The phase term is proportional to the distance of travel along the ray and, the proportionality constant in free space is the wave number, K_0. The amplitude term is derived in accordance with the optical form of the principle of conservation of energy in a narrow tube of rays emanating from a small region of the wavefront, as shown by Keller[2] for the various types of waves.

The rays incident on a dielectric scatterer are straight lines extending from the source. For the case of a finite scatterer, they suffer a unique number of reflections, diffractions and refractions. The field along all the resulting rays is determined by the particular path, as well as the properties of the source and the scattering body. The reflected and transmitted fields may be computed with the aid of reflection and transmission coefficients once these rays are properly identified and classified. Thus fora point of reflection:

$$U_r(P) = \sum_j U_i(Q_j)\ R(Q_j)\ e^{jK_oS} \qquad (1.1.1)$$

where $R(Q_j)$ is the reflection ceofficient at the point of reflection "Q_j", and $U_i(Q_j)$ is the incident field at "Q_j". The distance "S" is measured from "Q_j" to "P" .

Diffracted rays are treated in a slightly different manner. To illustrate this, consider the case of an incident ray tangent to the surface of a curved body shown in Fig. (1.1.1). The field on the incident ray at Q on the surface is:

$$U_i(Q) = A_i(Q)\ e^{jK_o\ \Psi_i(Q)} \qquad (1.1.2)$$

where A_i is the amplitude of the incident ray, and $K_o\ \Psi_i$ is the phase in radians. The field on the surface diffracted ray excited at Q due to this incident ray, may be expressed as:

$$U_d(Q) = A_d(Q)\ e^{jK_o\ \Psi_d(Q)} \qquad (1.1.3)$$

The phase terms, Ψ_i and Ψ_d are assumed equal at Q while the diffracted field is assumed proportional to the incident field at Q. Thus

$$A_d(Q) = D(Q)\ A_i(Q) \qquad (1.1.4)$$

where D(Q) is the diffraction coefficient which depends on the nature of the field, the surface properties of the object at Q (conductivity and dielectric constant), as well as the propagation constant K_o . The diffraction coefficient D(Q) is also dependent on whether Q is an edge, vertex or a surface point.

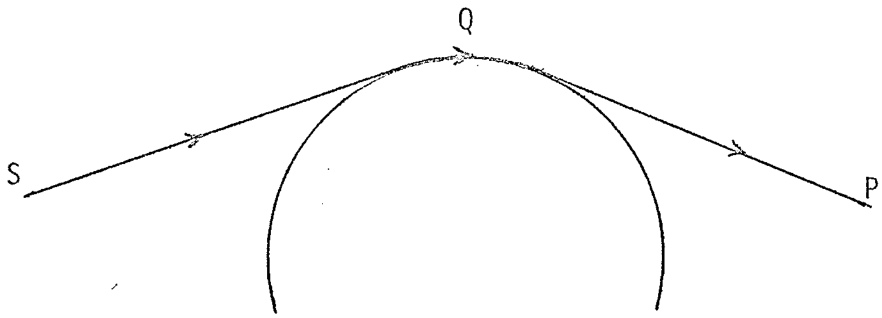

FIGURE (1.1.1)

A SURFACE DIFFRACTED RAY

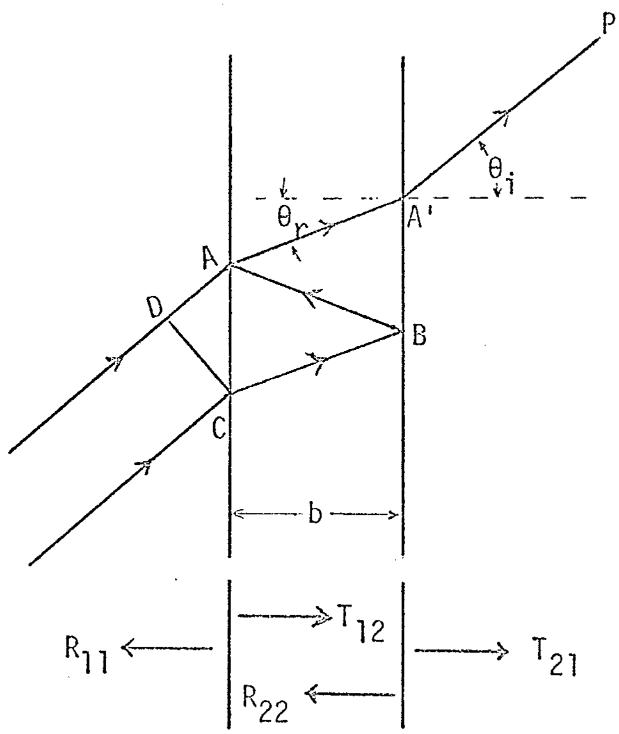

FIGURE (1.2.1)

RAYS TRANSMITTED THROUGH A DIELECTRIC SLAB

1.2 Application to a Lossless Dielectric Slab

Consider a plane wave obliquely incident on an infinite, homogeneous, dielectric slab of thickness, b, dielectric constant, ε_r, and with the electric field perpendicular to the plane of Fig. (1.2.1). The transmitted field is to be determined and compared with the available exact solution. The phase reference is taken as that of the fundamental ray, AA'P which traverses the slab once before reaching P. The ray which is reflected twice in the dielectric before emerging at P is shown as CBAA'P, will be ahead in phase compared to the fundamental ray. The difference in optical path length, ΔL, is given by

$$\Delta L = N(AB + BC) - AD,$$

where $$N^2 = \varepsilon_r \, .$$

But $$AB = BC = b/\cos\theta_r \, ,$$

$$AD = AC \sin\theta_i = 2b \tan\theta_r \sin\theta_i \, ,$$

where $$\theta_i = \text{angle of incidence},$$

$$\theta_r = \text{angle of refraction},$$

and $$\sin\theta_i = N \sin\theta_r \qquad \text{(Snell's Law)}$$

$$AD = 2b \tan\theta_r \quad N \sin\theta_r$$

$$\Delta L = N\, 2b/\cos\theta_r - 2b\, N \tan\theta_r \sin\theta_r$$

$$= 2\, N\, b \cos\theta_r \tag{1.2.1}$$

The phase lag due to a ray crossing the slab once is:

$$\delta = \frac{K_o\, \Delta L}{2} = \frac{2\pi\, N\, b \cos\theta_r}{\lambda} \tag{1.2.2}$$

By the method of images[3], there are an infinite number of secondary rays originating at the plane wave front which pass through P after a unique number of reflections. Each differs in phase from the fundamental by 2 n δ where n is an integer greater than zero. In the absence of the slab, the electric field at P is given by

$$E(P)_i = e^{-j K_o \Psi_o} \tag{1.2.3}$$

where the amplitude is normalized to unity and Ψ_o is a new phase reference calculated at P. As the slab is lossless, the amplitude reduction is due to the multiple reflections at both interfaces of the slab. Next define the wave matrix coefficients R_{11}, R_{22}, T_{12} and T_{21} as follows:

R_{11} = reflection coefficient at the free space-dielectric interface,

R_{22} = reflection coefficient at the dielectric-free space interface,

T_{12} = transmission ceofficient through the free space-dielectric interface = $1 + R_{11}$,

T_{21} = transmission coefficient through the dielectric-free space interface = $1 + R_{22}$.

The field at P due to the fundamental ray is:

$$[E(P)]_{n=o} = T_{12}T_{21}\, e^{j\delta}\, e^{-jK_o\Psi_o}$$

$$= T_{12}T_{21}\, e^{j\delta}\, E(P)_i \tag{1.2.4}$$

The field at P due to a secondary ray reflected twice is:

$$[E(P)]_{n=1} = T_{12}T_{21}\, R_{22}^2\, e^{j3\delta}\, E(P)_i \tag{1.2.5}$$

while the field at P due to n transmitted rays is:

$$\sum_{n=o} [E(P)]_n = T_{12}T_{21}\{e^{j\delta} + R_{22}^2\, e^{j3\delta} + R_{22}^4\, e^{j5\delta} + \dots$$

$$+ R_{22}^{2(n-1)}\, e^{j(2n-1)\delta}\}\, E(P)_i$$

$$= \left[T_{12}T_{21}\left(\frac{1 - R_{22}^{2n}\, e^{j2n\delta}}{1 - R_{22}^2\, e^{2j\delta}}\right) e^{j\delta}\right] E(P)_i\,. \tag{1.2.6}$$

For $n \to \infty$, Equation (1.2.6) becomes:

$$E(P) = E(P)_i \left[\frac{T_{12}T_{21}}{1 - R_{22}^2 \, e^{j2\delta}} \right] e^{j\delta} \qquad (1.2.7)$$

Stratton[4] has shown the solution of the boundary value problem for the special case of a plane wave normally incident on a dielectric slab. The result given for the transmission field may be expressed using the above notation, as follows:

$$E(P) = \frac{4\,E(P)_i}{(1 - Z_{12})(1 - Z_{21})\, e^{j\delta} + (1 + Z_{12})(1 + Z_{21})}\, e^{-j\delta} \qquad (1.2.8)$$

where $Z_{12} = N$, $Z_{21} = \frac{1}{N}$, and $R_{22} = (\frac{N-1}{N+1})$. On substituting for Z_{12} and Z_{21} and simplifying, there results:

$$E(P) = E(P)_i \left[\frac{T_{12}T_{21}}{1 - R_{22}^2 \, e^{j2\delta}} \right] e^{j\delta} \qquad (1.2.9)$$

which is identical to the result previously derived by the ray method.

1.3 Application to a Convex Cylinder

The geometrical theory of diffraction has been applied by Keller to an infinitely conducting cylinder[5,6] . Each incident ray in Fig. (1.3.1) which is tangent to the cylinder, gives rise to a diffracted ray. The diffracted rays produced in this manner, travel around the surface of the cylinder as surface rays. At any point on the cylinder surface, a diffracted ray splits off from each of the surface rays along the tangent to the cylinder, as shown in Fig. (1.3.2). Each of the diffracted rays split off from the surface ray, consists of an infinite number of diffracted rays which have encircled the cylinder different numbers of times.

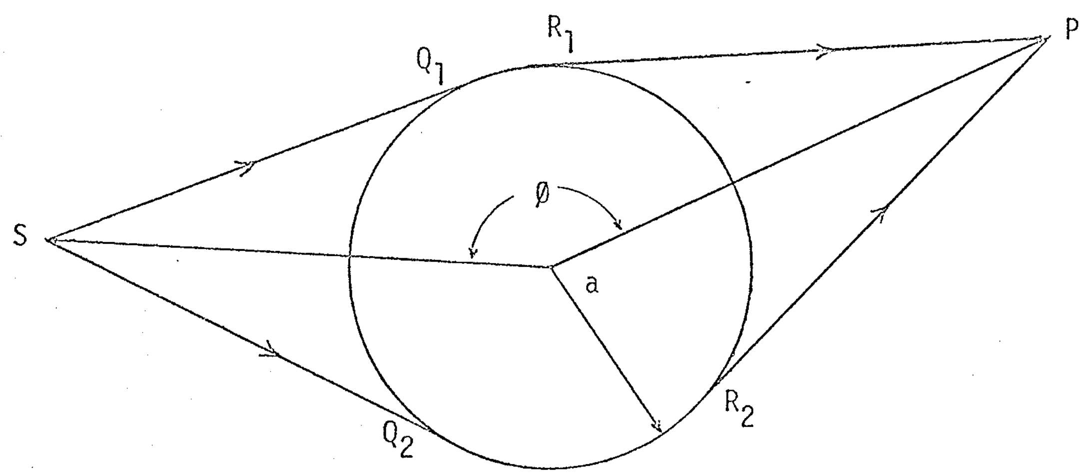

FIGURE (1.3.1)

RAYS DIFFRACTED AROUND A CYLINDER

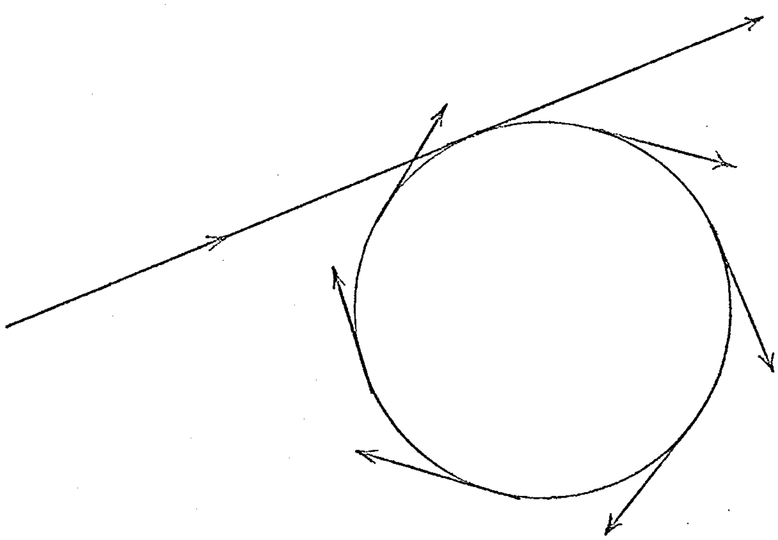

FIGURE (1.3.2)

DIFFRACTED RAYS EXCITED BY A SURFACE RAY

The diffracted rays passing through an observation point, P, are the tangent rays from the cylinder to P. The field determined by Keller[5] is:

$$U(r,\emptyset) \sim 0\left[\frac{D_s^{\,2}\, e^{-\alpha_s t}}{\sqrt{K_0}}\right]$$

where D_s is the diffraction coefficient, α_s is decay exponent due to radiation and t is the length of travel of the ray on the cylinder. This is compared to the leading term of the asymptotic expansion of the exact solution and the constants D_s and α_s are evaluated.

1.4 Conclusion

Keller's Theory has been tested mathematically for a great number of problems where rigorous or exact solutions are available[5,6,7]. In particular, the ray diagrams for the reflected, refracted and diffracted rays have been established for problems similar to the case of the dielectric cylinder. The geometrical optics ray diagrams for the dielectric cylinder, will be further established by another method. It is expected that the diagrams for the refracted and diffracted rays, as will be shown in later chapters, are correct and should lead to a reasonable agreement with published results where forward transmitted field data is available.

CHAPTER II

DIFFRACTION BY A DIELECTRIC CYLINDER

2.1 Introduction

In this chapter, the geometrical theory of diffraction is extended and applied to the problem of diffraction by an infinitely long dielectric cylinder. The incident electric field is polarized parallel to the axis of the cylinder since it is due to a z-directed line source located at the cylindrical co-ordinates $(r_o, \emptyset_o)$. For the perpendicular polarization case, the ray method is still valid since H_z rather than E_z is then considered. For the more general case of oblique polarization, the solution is obtained as the superposition of the parallel and perpendicular cases in exactly the same manner as shown by Burke and Keller[8].

2.2 Calculation of the Geometrical Optics Field

The scalar field produced by a time varying line source parallel to an infinite dielectric cylinder in free space, is determined using the ray method. The basic parameters of the cylinder are the radius, "a" and the index of refraction N , where

$$N = (\varepsilon_r)^{1/2} = \frac{K_1}{K_o} > 1 \tag{2.2.1}$$

and K_1/K_o is the ratio of the wave number in the cylinder to that in free space. The observation point where the field is desired, is assumed to be at $(r,\emptyset)$ with the center of the cylinder taken as the origin of the cylindrical co-ordinates. Furthermore, if the origin of the polar angle is measured away from the vector r_o , then $\emptyset_o = o$ and $\emptyset$ is the angle between the vectors r_0 and r measured in a clockwise sense.

In order to calculate the field $U(r,\emptyset)$ at point P , a ray diagram showing the incident, reflected, diffracted and refracted rays must be traced. Since this field is the sum of the fields on all the rays passing through P , the calculations may be presented in a step-wise manner. The resulting solution must, however, satisfy:

(a) the boundary conditions at the surface $(a,\emptyset)$, which require that the tangental components, (E_z,H_z), are both continuous;

(b) the Fresnel laws of reflection and refraction[4], and must also take into account the multiple reflections within the cylinder that account for the radiation component of the field.

2.2.1 Incident Rays

For certain values of r_0, r, a and $\emptyset$, the incident rays may reach the point P directly, as shown in Fig. (2.2.1). For such cases, the incident field U_i , is calculated using the optical form of the principle of conservation of energy. The principle states that in a time periodic field, the flux of energy is the same at all points in a narrow tube of rays[5]. The flux is proportional to the square of the field amplitude multiplied by the cross-sectional area of the tube, and by the velocity of propagation at that point. For a cylindrical wave, the distance between a pair of neighboring rays is $R_i\, d\Omega$, where R_i is the distance from the source, and $d\Omega$ is the angle between the two rays. The amplitude, $A(P)$, satisfies the relation:

$$A^2(P)\ R_i\ d\Omega = A_0^2\ d\Omega \qquad (2.2.2)$$

where A_0 is the amplitude on the ray in question at unit distance from the

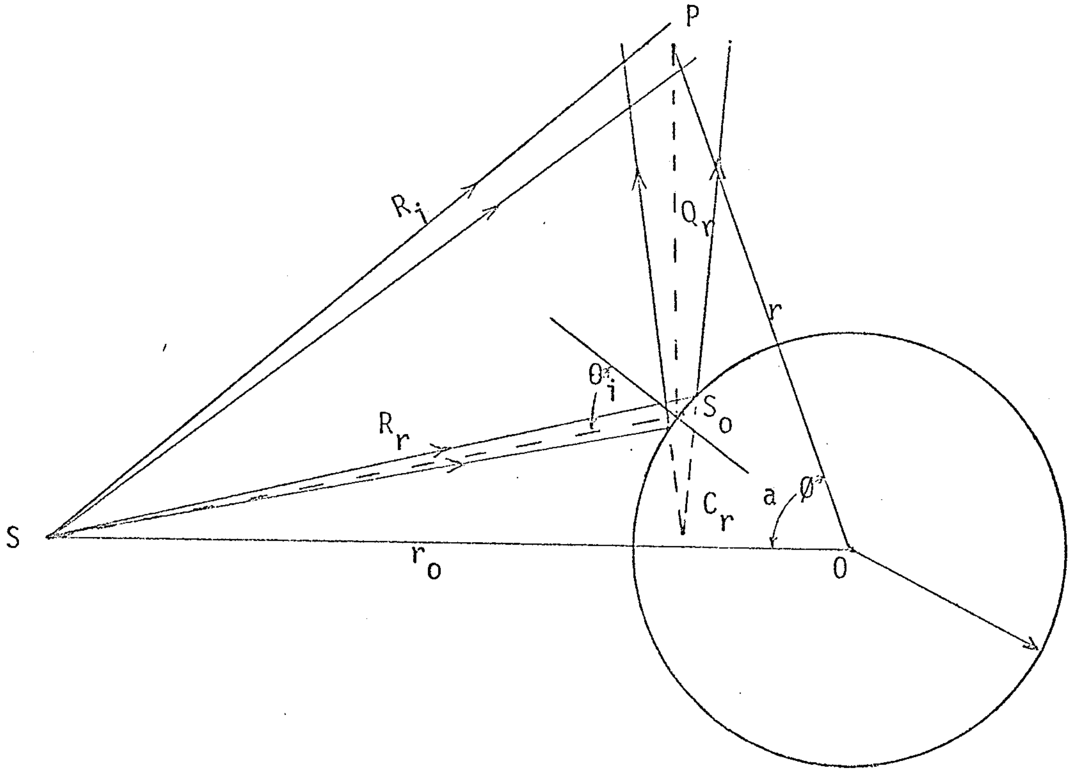

FIGURE (2.2.1)

INCIDENT AND REFLECTED RAYS

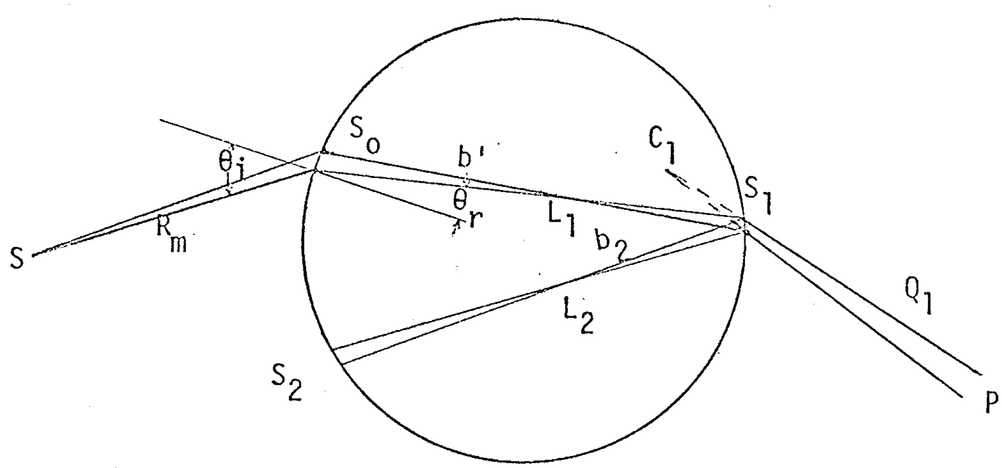

FIGURE (2.2.2)

RAYS REFRACTED THROUGH THE CYLINDER

source. Thus

$$A(P) \sim \frac{A_o}{\sqrt{R_i}} \tag{2.2.3}$$

To adjust the incident field to be that of a source of unit strength, Equation (2.2.3) is compared to the leading term of the asymptotic expansion of the function $H_o^{(1)}(K_o R_i)$ for a line source. This leads to

$$A_o = \sqrt{\frac{j}{8\pi K_o}} \tag{2.2.4}$$

The phase factor is $e^{jK_o R_i}$. The field due to the incident rays is thus:

$$U_i \sim \frac{A_o}{\sqrt{R_i}} e^{jK_o R_i} \tag{2.2.5}$$

where $R_i = (\gamma_o^2 + r^2 - 2\gamma_o\, r \cos \emptyset)^{1/2}$.

2.2.2 Reflected Rays

The contribution to the field at P due to the rays reflected from the surface, is found by considering a pair of neighboring reflected rays as shown in Fig. (2.2.1). When extended into the cylinder, these rays intersect at a distance C_r from the point of reflection, S_o. The cross-sectional area of the tube bounded by the two rays is $C_r\, d\Omega$ evaluated at the reflecting surface and $(C_r + Q_r)\, d\Omega$ at a distance Q_r from the point of reflection S_o along either ray. Thus, in the limit the amplitude of the reflected field at P due to a ray from S_o is:

$$A^2_{(P)}\, (Q_r + C_r)\, d\Omega = \frac{A_o^2}{R_r}\, C_r\, d\Omega$$

and

$$A(P) \sim \frac{A_o}{\sqrt{R_r}\, \sqrt{1 + \frac{Qr}{Cr}}} \tag{2.2.6}$$

where R_r = distance from the source to reflection point, S_o

$$= (r_o^2 - a^2 \sin^2 \theta_i)^{1/2} - a \cos \theta_i ,$$

Q_r = distance from the reflection point, S_o to P ,

$$= (r^2 - a^2 \sin^2 \theta_i)^{1/2} - a \cos \theta_i$$

and
$$\frac{1}{C_r} = \frac{2}{a \cos \theta_i} + \frac{1}{R_r} \tag{2.2.7}$$

as shown in Appendix (A2.1). The phase factor of the field is $e^{jK_o(R_r+Q_r)}$ while the complete expression for the field at P due to the reflected rays is

$$U_r \sim A_o R_{11} M_r R_r^{-1/2} e^{jK_o(R_r+Q_r)} \tag{2.2.8}$$

where
$$M_r = (1 + \frac{Q_r}{C_r})^{-1/2}$$

2.2.3 Refracted Rays

The field due to the rays which enter the cylinder and are internally reflected m-1 times before being refracted out to the field point, are shown in Fig. (2.2.2). Applying the energy principle again to the portion of this discontinuous ray from S_o to S_1 , there results:

$$A_{S_1}^2 (L_1 - b_1) \, d\,\Omega = \frac{A_o^2}{R_1} b_1 \, d\,\Omega ,$$

hence
$$A_{S_1} = \frac{A_o}{\sqrt{R_1}} \sqrt{\frac{b_1}{L_1 - b_1}}$$

$$= \frac{A_o}{\sqrt{R_1} \sqrt{\frac{L_1}{b_1} - 1}} \tag{2.2.9}$$

where A_{S_1} denotes the amplitude at S_1 , R_m is the distance from the source to S_o of the ray which traverses the cylinder m times before arriving at P,

L_m is the chord length from S_m-1 to S_m, and b_i is the distance from S_m-1 to the point of convergence of two neighboring rays along L_m. However, the convergence of two adjacent rays within the cylinder leads to a caustic or a phase lag of $\pi/2$ as shown by Kay and Keller[10]. This phase factor may be taken into account by mulitiplying the amplitude A_{S_1} by the term $e^{-j\,\pi/2}$, i.e.,

$$A_{S_1} = \frac{A_o}{\sqrt{R_1}\;\sqrt{1 - \frac{L_1}{b_1}}} \tag{2.2.10}$$

since $e^{-j\,\pi/2} = 1/j$. Similarly, when the energy principle is applied to the ray path from S_1 to S_2, and S_m-1 to S_m, the resulting amplitude is multiplied by the factors; N_1, N_2, ... N_m, where

$$N_i = \left(1 - \frac{L_i}{b_i}\right)^{-1/2} \qquad i = 1,2,... \tag{2.2.11}$$

The amplitude factor for the ray path from S_m to P is:

$$M_m = \left(1 + \frac{Q_m}{C_m}\right)^{-1/2} \tag{2.2.12}$$

where Q_m is the distance from S_m to P, and C_m is the distance from S_m to the point of convergence of two neighboring rays along Q_m.

The field produced at the external point due to a ray which is reflected (m - 1) times within the dielectric is given by:

$$U_m(r,\emptyset) \sim A_o\, N_1\, N_2 \ldots N_m\, M_m\, (R_m)^{-1/2}\, T_{12}\, T_{21}\, R_{22}^{m-1}$$
$$e^{j K_o(R_m + Q_m) + j K_1 \sum_{i=1}^{m} L_i} \tag{2.2.13}$$

where $T_{12}T_{21}\, R_{22}^{m-1}$ is an amplitude factor less than unity, resulting from the transmission into and out of the cylinder as well as the m-1 internal reflections.

The field produced by all the refracted rays is:

$$\sum_{m=1}^{\infty} U_m (r,\phi), \; r > a \quad 0 < |\phi| < 2\pi \tag{2.2.14}$$

in which the constants are determined from the geometric considerations shown in Appendix (A2.2) and Appendix (A2.3), as:

$$\frac{1}{b_1} = \frac{1}{a \cos \theta_r} \left[1 - \frac{\cos \theta_i}{N \cos \theta_r} - \frac{a \cos^2 \theta_i}{N R_1 \cos \theta_r} \right] , \tag{2.2.15}$$

$$\frac{1}{b_i} = \frac{2}{a \cos \theta_r} - \frac{1}{L-b_{i-1}} \qquad i = 2,3,4\ldots \tag{2.2.16}$$

$$\frac{1}{C_m} = \frac{\cos \theta_r}{\cos \theta_i} \left[\frac{N \cos \theta_r}{(L-b_m) \cos \theta_i} - \frac{N}{a \cos \theta_i} + \frac{1}{a \cos \theta_r} \right] , \tag{2.2.17}$$

and

$$L = L_i = 2 a \cos \theta_r \qquad i = 1,2,3,\ldots \tag{2.2.18}$$

Furthermore, since the ray path is completely defined by these relations, it is obvious that for any given line source, observation point and cylinder, there results a relation between ϕ and θ_i such that the unique value of θ_i may be determined from the following transcedental equation:

$$2\pi F_m \pm \phi = 2 \theta_i + m (\pi - 2 \theta_r) - \sin^{-1} \left(\frac{a}{r} \sin \theta_i\right) - \sin^{-1} \left(\frac{u}{r_0} \sin \theta_i\right) \tag{2.2.19}$$

where F_m is the smallest possible integer such that equation (2.2.19) has real solutions. The solution of this equation is best obtained by graphical methods as shown in Appendix (A4.1).

For the sake of convenience, Table (2.2.1) shows the various types of rays reaching the field point P. In this analysis, the m^{th} ray arriving at the field point, contains no contributions from reflections of higher order than m which might occur before the higher order ray is refracted to the field point.

TABLE (2.2.1)

GEOMETRIC RAY TYPES (W_{ij}) AT THE FIELD POINT*

Lit Region

RAY TYPE	REFRACTIONS NO. OF	REFLECTIONS NO. OF	AMPLITUDE MULTIPLIED BY
Incident	0	0	1
Reflected	0	1	R_{11}
Refracted m=1	2	0	$T_{12}\ T_{21}$
Refracted m=2	2	1	$T_{12}\ T_{21}\ R_{22}$
Refracted m	2	m-1	$T_{12}\ T_{21}\ R_{22}^{m-1}$

Shadow Region

RAY TYPE	REFRACTIONS	REFLECTIONS	AMPLITUDE FACTOR
Refracted m=1	2	0	$T_{12}\ T_{21}$
Refracted m=2	2	1	$T_{12}\ T_{21}\ R_{22}$
Refracted m	2	m-1	$T_{12}\ T_{21}\ R_{22}^{m-1}$

* i = no. of refractions   j = no. of reflections

2.3 Diffracted Ray Fields

For a dielectric cylinder with $N>1$, a diffracted ray can be produced only by an incident ray which is tangential to the boundary surface[5,6]. In order to satisfy the boundary condition of the problem, each tangent ray splits into three new rays at the point of tangency. One ray continues along the path of the incident ray; and another ray travels along the outer surface of the cylinder as a surface ray. The third ray is critically refracted into the cylinder and leads to higher order reflected, diffracted and refracted rays.

2.3.1 Types of Diffracted Rays

A field point may have infinitely many diffracted rays passing through it, as shown in Fig. (2.3.1). There are four main types of such rays which will now be discussed:

(1) Rays which start from the source, hit the cylinder tangentially, travel along the surface on the exterior side, and leave the surface tangentially to A.

(2) Rays emanating from the source which hit the cylinder tangentially, travel along the surface, are critically refracted into the cylinder, traverse the cylinder, hit the other side, are critically refracted, travel along the surface, and finally leave tangentially toward B.

(3) Rays of type (2) except that when they hit the other side of the cylinder, instead of being critically refracted, they are reflected back through the cylinder, hit another side, are critically refracted, travel along the exterior surface, and finally leave the surface tangentially to C.

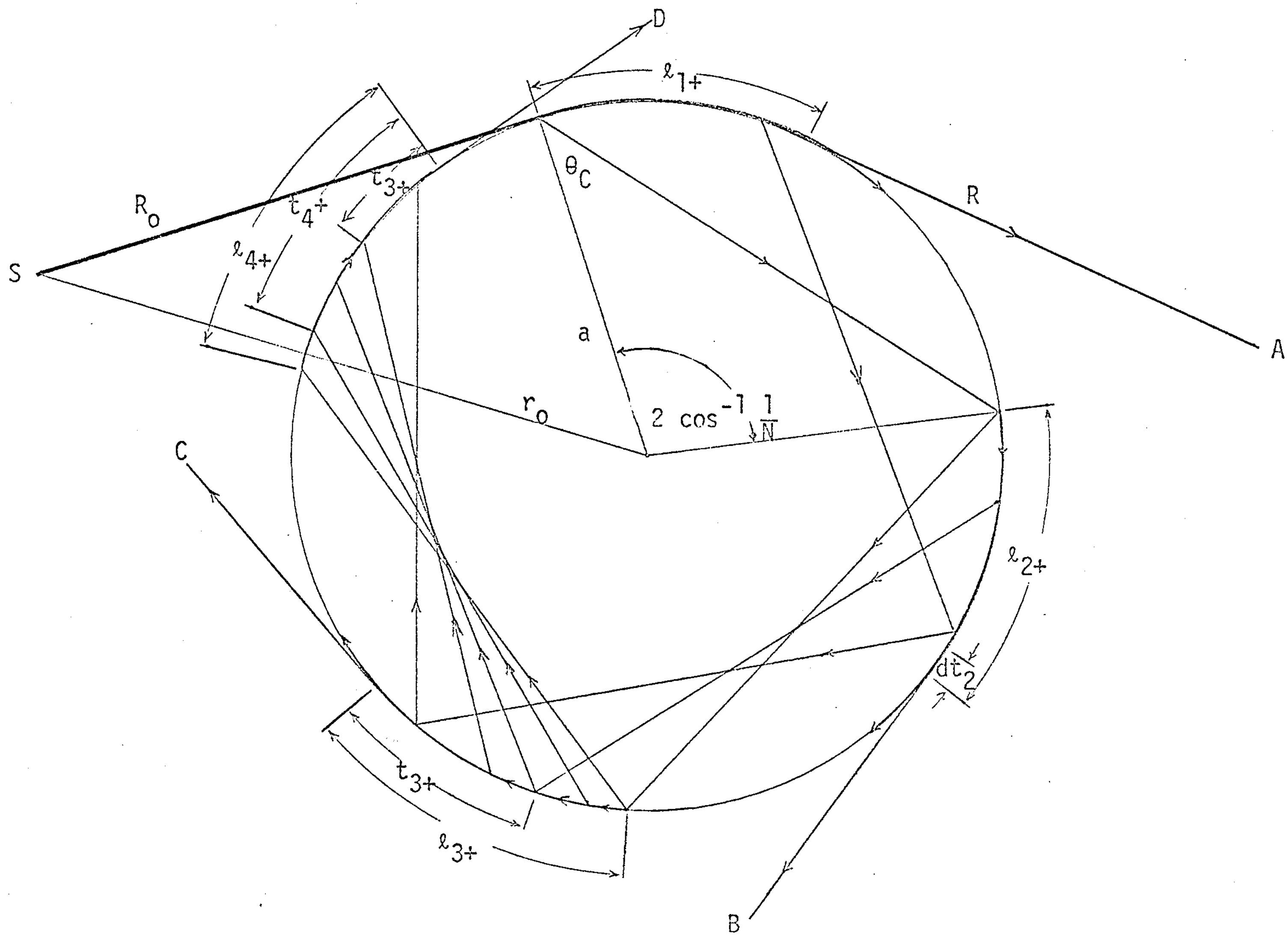

FIGURE (2.3.1)

TYPES OF DIFFRACTED RAYS

(4) Rays of type (2) except that when they travel along the surface, instead of leaving tangentially, they are critically refracted again into the cylinder, traverse the cylinder, are critically refracted, travel along the surface and finally leave tangentially.

The remainder of the diffracted rays are similar to the rays of the third and fourth kinds except with higher numbers of traversals of the cylinder which are due to either reflection or refraction.

For a surface portion of the diffracted ray, the phase of the field increases in proportion to the optical length of the ray. In travelling along the surface, the amplitude of the ray decreases due to radiation from the surface. The boundary surface is a caustic of the diffracted fields. The field within the caustic layer is composed of a number of different modes. Each mode is characterized by its own amplitude, and therefore its own diffraction coefficient and proportionality constant[5,6]. The constant given in (1.1.4) would thus express the diffraction due to one mode while the total diffracted field would be summed over all modes. The amplitudes of the four types of rays, however, decreases exponentially indicating that the surface modes are evanescent and their contribution is therefore numerically small compared to the incident, reflected and first order refracted rays.

2.3.2 Diffracted Field Calculations

To construct the diffracted fields due to a dielectric cylinder, let D_{11} , D_{12} and D_{21} be the diffraction coefficients for the field on rays travelling in free space, from free space to dielectric and from dielectric to free space respectively. Furthermore, define the angle of critical incidence as $\theta_c = \sin^{-1} 1/N$, and $\frac{\nu_s}{a}$ as the propagation constant along the boundary surface with s denoting the mode number. Since the wave is propagating in free-space, the real part of the ν_s/a is approximately equal to K_o ; and since the surface rays suffer an exponential decrease in amplitude, the imaginary part of ν_s/a (i.e. the decay exponent), is positive.

The field due to the rays which creep a distance ℓ_{o+} around the cylinder in a clockwise direction, or the distance ℓ_{o-} in a counter-clockwise direction are:

$$U_1 n\pm\ (r,\emptyset) \sim \sum_s A_o\, D_{11s}^2\ (R\, R_o)^{-1/2}\, e^{jK_o(R+R_o) + j\frac{\nu_s}{a}\ell_{1+}}$$

$$r>a \quad 0\leq\emptyset\leq 2\pi \qquad (2.3.1)$$

where $\ell_{1+} = a(2\pi n \pm \emptyset - \cos^{-1}\frac{a}{r} - \cos^{-1}\frac{a}{r_o})$

and n is any positive integer such that $\ell_{1\pm} \geq 0$,

$$R = (r^2 - a^2)^{1/2} \qquad R_o = (r_o^2 - a^2)^{1/2}$$

The total contribution of rays of this type is the sum of (2.2.1) over all possible values of n .

The contribution at an observation point due to type (2) rays is due to rays diffracted at all points along the whole arc of length ℓ_{2+} where

$$\ell_m = a\ (2\pi n \pm \emptyset - \cos^{-1}\frac{a}{r_o} - \cos^{-1}\frac{a}{r} - 2m\cos^{-1}\frac{1}{N})$$

$$m = 1,2,3...$$

To sum over these rays, the factor $\int_0^{\ell_{2+}} \frac{dt_{2+}}{a}$ is introduced into the expression for $U_2\, n+ (r,\emptyset)$ and $\int_0^{\ell_{2-}} \frac{dt_{2-}}{a}$ is introduced into the expression for $U_2\, n- (r,\emptyset)$ where dt_2 is the infinitesimal arc length measured from the point of tangency of the ray B to the point of second refraction of U_2 . The diffracted field at B is

$$U_2\, n\pm(r,\emptyset) \sim \sum_s A_o D_{11s}^2 D_{12} D_{21} (R R_o)^{-1/2} \int_0^{\ell_{2\pm}} \frac{dt_{2\pm}}{a} e^{jK_o(R+R_o) + j\, 2K_1\, a \cos\theta_C + j \frac{\nu s}{a} \ell_{2\pm} - j\pi/2}$$

$$\text{for} \quad r>a \qquad 0 \leq |\emptyset| \leq 2\pi \tag{2.3.2}$$

where $2\, K_1\, a \cos\theta_C$ is the chord length of the ray in the dielectric and $e^{-j\pi/2}$ accounts for the caustic due to the rays travelling along the chord.

The third and fourth kinds of rays are also shown in Fig. (2.2). Here the amplitude contains the factors, $R_{22} \int_0^{\ell_3} \frac{dt_3}{a}$ and $\int_0^{\ell_3} \frac{D_{12}D_{21}}{a} \times \left(\int_0^{t_3} \frac{dt_2}{a}\right) dt_2$, respectively, where dt_2 is the infinitesimal arc length measured from the point of tangency toward the third point of refraction of U_3 ; t_3 is the arc length measured from the point of tangency of the ray from C to the third point of refraction of U_3 ; dt_3 is the infinitesimal variation of t_3 measured from t_3 to the second point of refraction (second internal reflection point). This field contribution is:

$$U_3 n\pm\, (r,\emptyset) \sim \sum_s A_o D_{11s}^2 D_{12} D_{21} (R_o R)^{-1/2} \int_0^{\ell_{3+}} \left(R_{22} + D_{12}D_{21} \int_o^{t_3} \frac{dt_2}{a}\right) \frac{dt_3}{a}\, e^{jK_o(R+R_o) + j4K_1\, a\cos\theta_C + j\, \nu_s/a\, \ell_{3\pm} - j\pi} \tag{2.3.3}$$

The higher terms due to multiple reflections and refractions, lead to small contributions with amplitude factors of $R_{22}^2 \int_0^{\ell_{4\pm}} \frac{dt_4}{a}$ and

$$\int_0^{\ell_{4\pm}} \frac{D_{12}D_{21}}{a} \left[\int_0^{t_4} (R_{22} + D_{12}D_{21} \int_0^{t_3} \frac{dt_3}{a}) \frac{dt_3}{a}\right] \frac{dt_4}{a}.$$

Hence, by the same consideration as before, this field contribution is given by:

$$U_{4\ n\pm}(r,\emptyset) = \sum_s A_o D_{11s}^2 D_{12} D_{21} (R R_o)^{-1/2}$$

$$\left[\int_0^{\ell_{4t}} \left\{R_{22}^2 + D_{12} D_{21} \int_0^{t_4} (R_{22} + D_{12} D_{21} \int_0^{t_3} \frac{dt_2}{a}) \frac{dt_3}{a}\right\} \frac{dt_4}{a}\right]$$

$$e^{jK_o(R + R_o) + jK_1 6 a \cos \theta_C + j \frac{\nu_s}{a} \ell_{4\pm} - j 3\pi/2} \tag{2.3.4}$$

The general expression for $U_{m\ n\pm}(r, \emptyset)$ is expressed using $\omega_{m\pm} = \frac{\ell_{m\pm}}{a}$ for angular distance, as:

$$U_{m\ n\pm}(r,\emptyset) \sim \sum_s A_o D_{11s}^2 D_{12} D_{21} (R R_o)^{-1/2}$$

$$\left[R_{22}^{m-1} \omega_{m\pm} + R_{22}^{m-2} \frac{D_{12}D_{21} \omega_{m\pm}^2}{2!} + R_{22}^{m-3} (D_{12}D_{21})^2 \frac{\omega_{m\pm}^3}{3!} + \ldots\right.$$

$$\left. + R_{22}^{m-1-K} (D_{12} D_{21})^K \frac{\omega_{m\pm}^{k+1}}{(K+1)!} + \ldots + (D_{12}D_{21})^{m-1} \frac{\omega_{m\pm}^m}{m!}\right]$$

$$e^{j K_o (R + R_o) + j 2m K_1 a \cos \theta_C + j \nu_s \omega_{m\pm} - j m\pi/2}$$

$$\text{for} \quad r>a, \quad 0 \leq (\emptyset) \leq 2\pi \tag{2.3.5}$$

The total diffracted field is the sum of $U_{m\ n\pm}(r, \emptyset)$ for all m.

CHAPTER III

COMPARISON WITH THE EXACT SOLUTION

The scattering from an infinitely long dielectric cylinder by a time-harmonic field due a line source, parallel to the axis of the cylinder, is investigated. The resulting field is expanded asymptotically as an infinite series of produces of radial and angular wave functions. The incident, reflected, transmitted, and multiply reflected fields are evaluated approximately using the saddle point method of integration. In addition, the diffracted fields are determined by the method of residues[11]. The procedure used is similar to that given by Streifer and Kodis[12] except for the comparison with the previous solution based on the geometrical theory of diffraction.

3.1 Exact Solution

The field $U(r,\emptyset)$ produced by an infinite line source with its electric vector parallel to the axis of a dielectric cylinder, is the solution of the following wave equation:

$$(\nabla^2 + K_0^2)\, U = -\delta\,(r - r_0)\,\frac{\delta(\emptyset)}{r} \qquad r \geq a \tag{3.1.1}$$

$$(\nabla^2 + K_1^2)\, U = 0 \qquad r \leq a \tag{3.1.2}$$

$$U(a^+,\emptyset) = U(a^-,\emptyset) \tag{3.1.3}$$

$$\frac{\partial\, U(a^+,\emptyset)}{\partial\, r} = \frac{\partial\, U(a^-,\emptyset)}{\partial\, r} \tag{3.1.4}$$

$$\lim_{r\to\infty} r^{\frac{1}{2}} \left(\frac{\partial U}{\partial r} - j\, K_0 U\right) = 0 \tag{3.1.5}$$

The resulting solution for the scalar field is evaluated in Appendix (A3.1) by the method of separation of variables. The result is:

$$U(r,\emptyset) = \frac{j}{4} \sum_{\nu=-\infty}^{\infty} e^{j\nu\emptyset} \Big[H_\nu^{(1)}(K_o r_>) \, J_\nu(K_o r_<)$$

$$- P_\nu H_\nu^{(1)}(K_o r_>) \, H_\nu^{(1)}(K_o r_<) \Big] \quad r \geq a \tag{3.1.6}$$

where $r_>$ refers to the maximum of (r,r_o), and $r_< = \min(r,r_o)$, and

$$P_\nu = \frac{J_\nu(K_1 a)\, J_\nu'(K_o a) - N\, J_\nu'(K_1 a)\, J_\nu(K_o a)}{J_\nu(K_1 a)\, H_\nu^{(1)'}(K_o a) - N\, J_\nu'(K_1 a)\, H_\nu^{(1)}(K_o a)} \tag{3.1.7}$$

The summation in (3.1.6) may be expressed in terms of a rapidly converging sum of integrals using the Poisson summation formula, thus:

$$U(r,\emptyset) = \frac{j}{4} \sum_{n=-\infty}^{\infty} \int_{-\infty}^{\infty} e^{j\nu(\emptyset + 2\pi n)} \Big[H_\nu^{(1)}(K_o r_>)\, J_\nu(K_o r_<)$$

$$- P_\nu H_\nu^{(1)}(K_o r_>)\, H_\nu^{(1)}(K_o r_<) \Big] d\nu \quad r \geq a \quad 0 \leq |\emptyset| \leq 2\pi \tag{3.1.8}$$

To obtain a physical interpretation of the equation, P_ν is expanded into a geometric series (see Appendix (A3.2)), as follows:

$$P_\nu = \frac{1}{2} \left\{ 1 - \frac{H_\nu^{(2)}(K_o a)}{H_\nu^{(1)}(K_o a)} \left[R_{11} + T_{12} T_{21} \sum_{m=1}^{\infty} R_{22}^{m-1} \left(\frac{H_\nu^{(1)}(K_1 a)}{H_\nu^{(2)}(K_1 a)} \right)^m \right] \right\} \tag{3.1.9}$$

using the logarithmic derivation functions[14];

$$R_{11} = - \left[\frac{\log' H_\nu^{(2)}(K_o a) - N \log' H_\nu^{(2)}(K_1 a)}{\log' H_\nu^{(1)}(K_o a) - N \log' H_\nu^{(2)}(K_1 a)} \right], \tag{3.1.10}$$

$$R_{22} = - \left[\frac{\log' H_\nu^{(1)}(K_o a) - N \log' H_\nu^{(1)}(K_1 a)}{\log' H_\nu^{(1)}(K_o a) - N \log' H_\nu^{(2)}(K_1 a)} \right], \tag{3.1.11}$$

where:

$$\log' H_\nu^{(j)}(z) = \frac{H_\nu^{(j)}(z)}{H_\nu^{(j)}(z)} \qquad j = 1,2 ,$$

$$T_{12} = 1 + R_{11} \qquad\qquad T_{21} = 1 + R_{22}$$

Substituting (3.1.9) into (3.1.8) leads to the result:

$$U(r,\emptyset) = \frac{j}{8} \sum_n \int_{-\infty}^{\infty} e^{j\nu(\emptyset+2\pi n)} \Bigg\{ 2\, H_\nu^{(1)}(K_o r_>) \;\; J_\nu(K_o r_<)$$

$$+ \left[R_{11} \frac{H_\nu^{(2)}(K_o a)}{H_\nu^{(1)}(K_o a)} - 1 \right] H_\nu^{(1)}(K_o r_>) \;\; H_\nu^{(1)}(K_o r_<) \; + \; T_{12} T_{21} \frac{H_\nu^{(2)}(K_o a)}{H_\nu^{(1)}(K_o a)}$$

$$\times \sum_{m=1}^{\infty} R_{22}^{m-1} \left(\frac{H_\nu^{(1)}(K_1 a)}{H_\nu^{(2)}(K_1 a)} \right)^m H_\nu^{(1)}(K_o r_>) \; H_\nu^{(1)}(K_o r_<) \Bigg\} \, d\nu$$

$$r \geq a \quad 0 \leq (\emptyset) \leq 2\pi \qquad\qquad (3.1.12)$$

By changing ν to $-\nu$, and using the identities:

$$H_{-\nu}^{(1)}(z) = e^{j\nu\pi}\, H_\nu^{(1)}(z) \; ,$$

$$H_{-\nu}^{(2)}(z) = e^{-j\nu\pi} H_\nu^{(2)}(z) \; ,$$

$$J_\nu(z) \quad = \frac{1}{2} \, [H_\nu^{(1)}(z) + H_\nu^{(2)}(z)] \; ,$$

equation (3.1.12) may be written as follows:

$$U(r,\emptyset) = \frac{j}{8} \sum_n \int_{-\infty}^{\infty} e^{j\nu[2\pi(1-n)-\emptyset]} \Bigg\{ H_\nu^{(1)}(K_o r_>) \;\; H_\nu^{(1)}(K_o r_<)$$

$$+ \, e^{-j2\nu\pi} \, H_\nu^{(1)}(K_o r_>) \, H_\nu^{(2)}(K_o r_<) \;\; -2P_{-\nu} H_\nu^{(1)}(K_o r_>) \; H_\nu^{(1)}(K_o r_<) \Bigg\} \, d\nu \qquad (3.1.13)$$

Since $\emptyset$ is subject to the restriction $0 \leq (\emptyset) \leq 2\pi$, then for $n \geq o$, only (3.1.12) will give a contribution to the field. Similarly, (3.1.13) represents the terms for $n < o$. These two equations may be written:

$$U(r,\emptyset) = \frac{j}{8}\left(\sum_{n=-\infty}^{-1} \int_{-\infty}^{\infty} e^{j\nu[2\pi(1-n)-\emptyset]} \left\{ H_\nu^{(1)}(K_o r_>)\, H_\nu^{(1)}(K_o r_<) \right.\right.$$

$$\left. + e^{-j2\pi\nu}\, H_\nu^{(1)}(K_o r_>)\, H_\nu^{(2)}(K_o r_<) - 2\, P_{-\nu} H_\nu^{(1)}(K_o r_>)\, H_\nu^{(1)}(K_o r_<) \right\} d\nu$$

$$+ \sum_{n=o}^{\infty} \int_{-\infty}^{\infty} e^{j\nu(\emptyset+2\pi n)} \left\{ 2\, H_\nu^{(1)}(K_o r_>)\, J_\nu(K_o r_<) + \left[R_{11} \frac{H_\nu^{(2)}(K_o a)}{H_\nu^{(1)}(K_o a)} - 1 \right] \right.$$

$$X\, H_\nu^{(1)}(K_o r_>)\, H_\nu^{(1)}(K_o r_<) + T_{12}T_{21} \frac{H_\nu^{(2)}(K_o a)}{H_\nu^{(1)}(K_o a)} \sum_{m=1}^{\infty} R_{22}^{\,m-1} \left(\frac{H_\nu^{(1)}(K_1 a)}{H_\nu^{(2)}(K_1 a)} \right)^m$$

$$\left.\left. X\, H_\nu^{(1)}(K_o r_>)\, H_\nu^{(1)}(K_o r_<) \right\} d_\nu \right)_{r \geq a} \quad 0 \leq |\emptyset| \leq 2\pi \qquad (3.1.14)$$

3.2 Geometric Optics Field

The scattered field is composed of a geometric optics field, and a diffracted field. The criterion for the identification of the geometric optics field from (3.1.14) is the existence of real saddle points, $\nu_{oj}(j = 1,2,\ldots)$ such that $0<|\nu_{oj}|< K_o\, r_<$. Each term of (3.1.14) is evaluated asymptotically in K_o and K_1 . Since the main contribution of the integrals comes from the range in which $|\mathrm{Re}\ \nu| < K_o r_<$, the Debye asymptotic forms of $H_\nu^{(1)}(K_o r_>)$ and $H_\nu^{(1)}(K_o r_<)$, given in Appendix (A3.3), are used. The resulting terms are identified with the corresponding ray terms given in the previous chapter.

3.2.1 The Incident Field

The first term of (3.1.14) is rewritten as:

$$U_i(r,\emptyset) = \frac{j}{B} \sum_n \Bigg[\int_{-\infty}^{\infty} e^{j\,(\emptyset+2\pi n)} \; H_\nu^{(1)}(K_o r_>) \, H_\nu^{(1)}(K_o r_<) \; d\,\nu$$

$$+ \int_{-\infty}^{\infty} e^{j\nu(\emptyset+2\pi n)} \; H_\nu^{(1)}(K_o r_>) \;\; H_\nu^{(2)}(K_o r_<) \; d\nu \Bigg] \quad r \geq a \;\; 0 \leq |\emptyset| \leq 2\pi \qquad (3.2.1)$$

When the Debye asymptotic forms of Appendix (A3.3) are substituted in the integrand, the resulting integral may be evaluated by the saddle point method as shown in Appendix (A3.4). The resulting infinite series has a real saddle point at n=0. The corresponding saddle point equations for the first and second integrals of (3.2.1) respectively, are:

$$\cos^{-1} \frac{\nu_o}{K_o\, r_>} + \cos^{-1} \frac{\nu_o}{K_o r_<} = \emptyset \qquad (3.2.2)$$

$$\cos^{-1} \frac{\nu_o}{K_o r_>} - \cos^{-1} \frac{\nu_o}{K_o r_<} = \emptyset \qquad (3.2.3)$$

Equation (3.2.2) has a real nonzero solution only in the unshaded region of Fig. (3.2.1), and (3.2.3) has a real nonzero solution only in the shaded region. The geometrical interpretation of $\frac{\nu_o}{K_o}$ is also shown in Fig. (3.2.1). The positive solutions of both (3.2.3) and (3.2.3) correspond to field points above the line OS. The negative solutions of the equations correspond to the field points below the line OS. The result obtained from evaluation by the saddle point method is:

$$U_i(r,\emptyset) \sim A_o \; (R_i)^{-\frac{1}{2}} \;\; e^{jK_oR_i} \quad r \geq a \quad 0 \leq |\emptyset| \leq 2\pi \qquad (3.2.4)$$

which is identical to (2.2.5) determined by the ray tracing method.

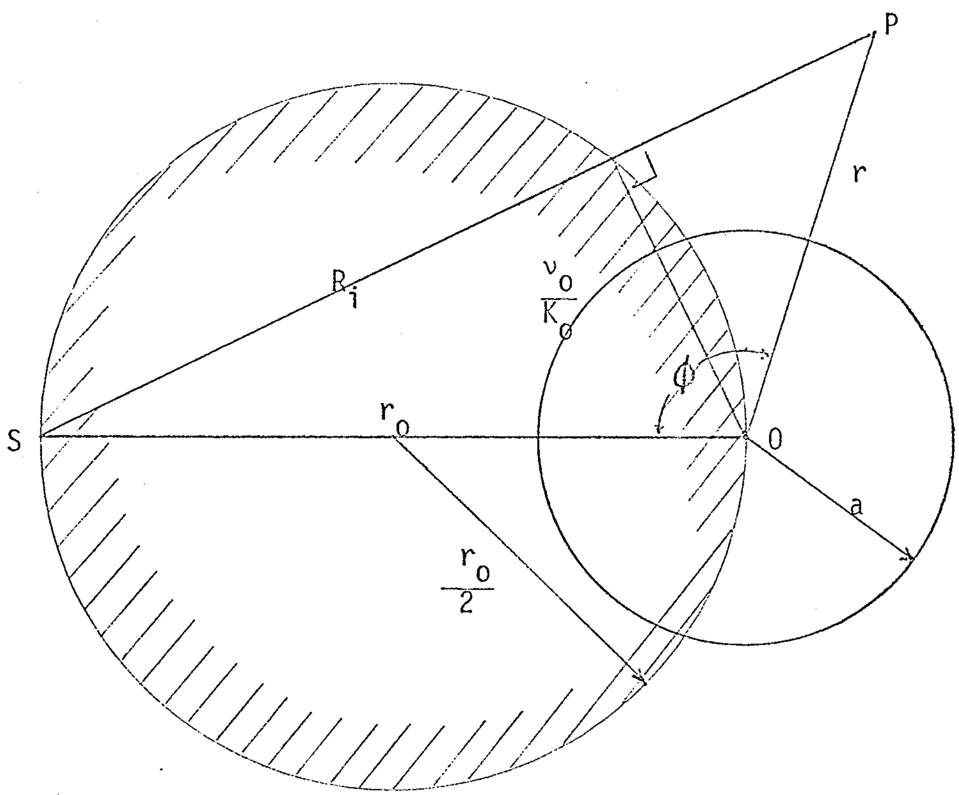

FIGURE (3.2.1)

GEOMETRICAL INTERPRETATION OF THE SADDLE POINT
OF THE INCIDENT RAY

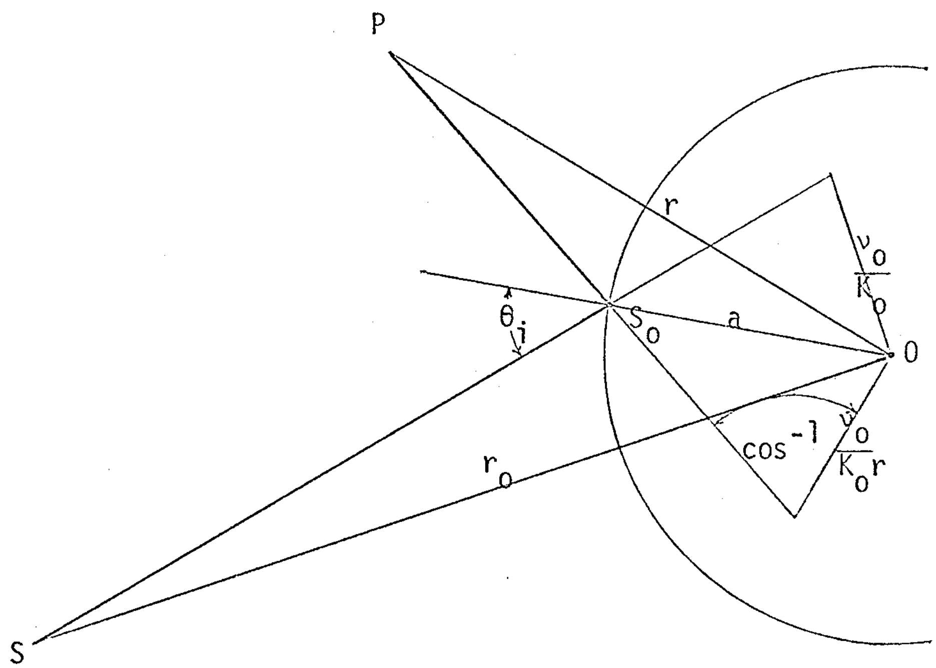

FIGURE (3.2.2)

GEOMETRICAL INTERPRETATION OF THE SADDLE POINT
OF THE REFLECTED RAY

3.2.2 Externally Reflected Field

The next term of (3.1.4) may be rewritten as:

$$U_r(r,\emptyset) = \frac{j}{8} \sum_n \int e^{j\nu(\emptyset+2\pi n)} \left[R_{11} \frac{H_\nu^{(2)}(K_o a)}{H_\nu^{(1)}(K_o a)} - 1 \right] H_\nu^{(1)}(K_o r_>) \, H_\nu^{(1)}(K_o r_<) \, d\nu$$

$$r \geq a \quad 0 \leq |\emptyset| \leq 2\pi \tag{3.2.5}$$

Since the second term in the integrand of (3.2.5) is the negative of the first term in the integrand of (3.2.1), they cancel out. However, the incident field in the unshaded area of Fig. (3.2.1) remains, as will now be shown. When the Debye asymptotic forms of the Hankel functions are substituted in the first term of the integrand of (3.2.5), two real saddle points result. One lies in the range, $0<|\nu_o|<K_o a$; and the other is in the range $K_o a<|\nu_o|<K_o r_<$. For the saddle point which satisfies the condition $K_o a<|\nu_o|<K_o r_<$, the identity $H_\nu^{(1)}(K_o a) \sim - H_\nu^{(2)}(K_o a)$ holds[16]. When substituted in the integrand, with R_{11} given by (3.1.10), there results:

$$R_{11} \frac{H_\nu^{(2)}(K_o a)}{H_\nu^{(1)}(K_o a)} \sim 1 ,$$

and the first integral of (3.2.5) is identical with the first integral of (3.2.1), giving the incident field in the unshaded area of Fig. (3.2.1).

The external reflected field is determined from the saddle point which satisfies the condition $0<|\nu_o|<K_o a$. The Debye asymptotic forms are substituted for all the Hankel functions in (3.2.5). The saddle point equation of any term in the infinite series of (3.2.5) is found in Appendix (A3.5) to be:

$$\cos^{-1} \frac{\nu_o}{K_o r_>} + \cos^{-1} \frac{\nu_o}{K_o r_<} - 2 \cos^{-1} \frac{\nu_o}{K_o a} = \emptyset + 2\pi n \tag{3.2.6}$$

As shown in Fig. (3.2.2), this equation has a positive real solution only for n=o , with the field point lying in the lit region above the line OS, and, has a negative real solution only for n=1 with the field point lying in the lit region below the line OS. The solution of (3.2.6), expressed in terms of the physical angle $\theta_i = \theta_i(r,r_o,\emptyset)$, is the physical angle $\theta_i = \theta_i(r,r_o,\emptyset)$, is

$$\nu_o = \pm K_o a \sin\theta_i \tag{3.2.7}$$

When (3.2.7) is substituted into (3.2.6) the resulting relation between $\emptyset$ and θ_i is:

$$\left\{\begin{array}{l} \emptyset \\ 2\pi - \emptyset \end{array}\right\} = 2\,\theta_i - \sin^{-1}\left(\frac{a}{r_o}\sin\theta_i\right) - \sin^{-1}\left(\frac{a}{r}\sin\theta_i\right) \tag{3.2.8}$$

which is similar to (2.2.19) obtained by the ray method. When (3.2.5) is evaluated asymptotically, the result shown in Appendix (A3.5) is:

$$U_r(r,\emptyset) \sim A_o\; R_{11}(R_r)^{-\frac{1}{2}}\; M_r\; e^{j(R_r+Q_r)} \tag{3.2.9}$$

which may be identified with the corresponding term in the ray solution, (2.2.8).

3.2.3 Higher Order Transmission Field

To find the field due to transmission through the cylinder, the following equation is evaluated asymptotically by the saddle point method:

$$U_m(r,\emptyset) = \frac{j}{8}\sum_n \int_{-\infty}^{\infty} e^{j\nu(\emptyset+2\pi n)}\, H_\nu^{(1)}(K_o r_>)\, H_\nu^{(1)}(K_o r_<)\, T_{12}T_{21}\, \frac{H_\nu^{(2)}(K_o a)}{H_\nu^{(1)}(K_o a)}$$

$$R_{22}^{\;m-1}\left(\frac{H_\nu^{(1)}(K_1 a)}{H_\nu^{(2)}(K_1 a)}\right)^m d\nu \quad r\geq a \quad 0\leq|\emptyset|<2\pi \quad m = 1,2,3\ldots \tag{3.2.10}$$

The saddle point equation is found in Appendix (A3.6) to be:

$$\cos^{-1}\frac{\nu_o}{K_o r_>} + \cos^{-1}\frac{\nu_o}{K_o r_<} + 2m\cos^{-1}\frac{\nu_o}{NK_o a} - 2\cos^{-1}\frac{\nu_o}{K_o a} = \emptyset + 2\pi n \qquad (3.2.11)$$

The positive solutions give the contributions of the field incident on the upper half of the cylinder, and the negative solutions give the contributions of the field incident on the lower half. When (3.2.7) is substituted into (3.2.10) the following result is obtained:

$$\left\{\begin{matrix} 2\pi F_m^+ + \emptyset \\ 2\pi F_m^- - \emptyset \end{matrix}\right\} = 2\theta_i + m(\pi - 2\theta_r) - \sin^{-1}\left(\frac{a}{r}\sin\theta_i\right)$$

$$- \sin^{-1}\left(\frac{a}{r_o}\sin\theta_i\right) \qquad (3.2.12)$$

where $\sin\theta_r = \frac{1}{N}\sin\theta_i$. This equation is valid only if either F_m^+ or F_m^- is determined as the smallest positive integer such that (3.2.12) has real solutions. This equation is identical with (2.2.19) obtained from the previous construction of geometrical optics rays.

The typical form of the contribution from any saddle point is shown in Appendix (A3.6) to be:

$$U_m(r,\emptyset) \sim A_o\, N_1 N_2 \ldots N_m M_m R_m^{-\frac{1}{2}}\, T_{12} T_{21}\, R_m^{m-1}$$

$$e^{jK_o(R_m+Q_m) + jK_1 \sum_{i=1}^{m} L_i} \qquad r \geq a \quad 0 \leq |\emptyset| \leq 2\pi \qquad (3.2.13)$$

which corresponds to (2.2.13) of the ray solution.

3.3 Diffracted Field

Any integral in (3.1.14) which does not have a real saddle point, may still be evaluated by the method of residues. When evaluated asymptotically, each integral leads to a contribution to the diffracted field. The expression (3.2.5) for $U_r(r,\emptyset)$, has simple poles in the integrand which may be determined from the equation:

$$\frac{H_\nu^{(1)'}(K_o a)}{H_\nu^{(1)}(K_o a)} - N \; \frac{H_\nu^{(2)'}(K_1 a)}{H_\nu^{(2)}(K_1 a)} = 0 \tag{3.3.1}$$

Similarly the expression (3.2.10) for $U_m(r,\emptyset)$ has poles of order m-1 . The approximate positions of the roots ν_s of (3.3.1) in the upper complex ν-plane are[6]:

$$\nu_s = K_o a + g_s \left(\frac{K_o a}{6}\right)^{1/3} e^{j\pi/3} + \ldots$$

where g_s is a number determined by substituting the Debye asymptotic forms of $H_\nu^{(2)'}(K_1 a)$ and $H_\nu^{(2)}(K_1 a)$, and the Airy function asymptotic forms of $H_\nu^{(1)'}(K_o a)$ and $H_\nu^{(1)}(K_o a)$, from Appendix (A3.3), into (3.3.1):

$$e^{j\pi/3} \left(\frac{6}{K_o a}\right)^{1/3} \frac{A'(g_s)}{A\,(g_s)} = j\,N \left[1 - \left(\frac{\nu_s}{K_1 a}\right)^2\right]^{1/2} \tag{3.3.2}$$

where A(z) is the Airy function[15].

Equation (3.2.5) can be written in two equivalent forms which will show their physical interpretation:

$$U_r(r,\emptyset) = \frac{j}{8}\int_{-\infty}^{\infty} e^{j\nu(\emptyset+2\pi n)} \; H_\nu^{(1)}(K_o r_>)\; H_\nu^{(1)}(K_o r_<) \left[R_{11} \frac{H_\nu^{(2)}(K_o a)}{H_\nu^{(1)}(K_o a)} - 1\right] d\nu$$

$$r \geq a \qquad 0 \leq |\emptyset| \leq 2\,\pi \tag{3.3.3}$$

is equivalent to:

$$U_r(r,\emptyset) = \frac{j}{8}\int_{-\infty}^{\infty} e^{-j\nu(\emptyset+2\pi n)} \; H_\nu^{(1)}(K_o r_>)\; H_\nu^{(1)}(K_o r_<) \left[R_{11} \frac{H_\nu^{(2)}(K_o a)}{H_\nu^{(1)}(K_o a)} - e^{j2\nu\pi}\right] d\nu$$

$$r \geq a \quad 0 \leq |\emptyset| \leq 2\pi \tag{3.3.4}$$

Similarly, the expression for $U_m(r,\emptyset)$,

$$U_m(r,\emptyset) = \frac{j}{8}\int_{-\infty}^{\infty} e^{j\nu(\emptyset+2\pi n)}\, T_{12}T_{21}\, R_{22}^{m-1}\, H_\nu^{(1)}(K_o r_>)\, H_\nu^{(1)}(K_o r_<)\, \frac{H_\nu^{(2)}(K_o a)}{H_\nu^{(1)}(K_o a)}$$

$$X\left(\frac{H_\nu^{(1)}(K_1 a)}{H_\nu^{(2)}(K_1 a)}\right)^m d\nu \quad r\geq a \quad 0\leq|\emptyset|\leq 2\pi \qquad (3.3.5)$$

is equivalent to:

$$U_m(r,\emptyset) = \frac{j}{8}\int_{-\infty}^{\infty} e^{j\nu[(m-n)2\pi -\emptyset]}\, T_{12}T_{21}\, R_{22}^{m-1}\, H_\nu^{(1)}(K_o r_>)\, H_\nu^{(1)}(K_o r_<)$$

$$X\ \frac{H_\nu^{(2)}(K_o a)}{H_\nu^{(1)}(K_o a)}\left(\frac{H_\nu^{(1)}(K_1 a)}{H_\nu^{(2)}(K_1 a)}\right)^m d\nu \quad r\geq a \quad 0\leq\emptyset\leq 2\pi \qquad (3.3.6)$$

3.3.1 First Order Diffracted Field

In order to evaluate $U_r(r,\emptyset)$, the Hankel functions, $H_\nu^{(1)}(K_o r_>)$, $H_\nu^{(1)}(K_o r_<)$, $H_\nu^{(1)}(K_1 a)$ and $H_\nu^{(2)}(K_1 a)$ are replaced by their Debye asymptotic forms, and $H_\nu^{(1)}(K_o a)$ and $H_\nu^{(2)}(K_o a)$ are replaced by their Airy Function asymptotic forms. Equation (3.3.3) is evaluated by the method of residues in Appendix (A3.7) where the terms of the order $\left[\frac{1}{K_o a\,(N^2-1)^{1/2}}\right]$ are neglected. The final result is:

$$U_r(r,\emptyset) \sim \sum_s A_o\, D_{11s}^2\, (R\, R_o)^{-1/2}\, e^{jK_o(R+R_o) + j\nu_s\omega_1 +}$$

$$r \geq a \quad 0<|\emptyset|<2\pi \qquad (3.3.7)$$

when compared to the result obtained by the ray method, (2.3.1), the diffraction coefficient is determined as:

$$D_{11s}^2 = \sqrt{\frac{2\pi}{K_o}}\ \pi(6)^{-2/3}\ e^{j\,5\pi/12}\,(K_o a)^{-1/3}\,[N^2-1]^{-1}\,[A(gs)]^{-2} \qquad (3.3.8)$$

A similar evaluation of (3.3.4) by the method of residues, yields

$$U_1(r,\emptyset) \quad \sum_s \; A_o \; D_{11s}^2 \; (R\, R_o)^{-1/2} \quad e^{jK_o(R+R_o) + j\, \nu_s \omega_{1-}} \tag{3.3.9}$$

For fixed values of $\emptyset$, r, r_o, a and n, (3.3.7) is used if, and only if, $\omega_{1+} \geq 0$, and (3.3.9) is used if, and only if, $\omega_{1-} \geq 0$. The two are mutually exclusive. Thus, when the field point lies in the shadow region, (3.3.7) is used for n = 0,1,2..., and (3.3.9) is used for n = -1,-2,... When the field point is situated in the upper lit region, (3.3.7) is used for n = 1,2,..., and (3.3.9) is used for n = -1,-2,-3... Also, when the field field point is situated in the lower lit region, (3.3.7) is used for n = 0,1,2... and (3.3.9) is used for n = -2,-3,... The missing terms give the geometric optics field in different lit regions as discussed previously. Physically, (3.3.7) represents the portion of the incident wave whose Poynting vector hits the upper surface of the cylinder tangentially. It decays exponentially while travelling clockwise along the cylinder surface for an angular distance ω_{1+} , and then leaves the surface tangentially toward the field point. Similarly, (3.3.9) represents the portion of the incident wave whose Poynting vector hits the lower surface of the cylinder tangentially. It also decays exponentially while travelling counter-clockwise for an angular distance ω_{1-} , and then leaves the surface tangentially toward P. For the sake of illustration, only the positive case is shown in Fig. (2.3.1).

3.3.2 Higher Order Diffracted Fields

In evaluating (3.3.5) the Hankel functions are again replaced by their Debye and Airy Function asymptotic forms. Equation (3.3.5) is evaluated in Appendix (A3.8) for m=1 and the result is:

$$U_2(r,\emptyset) \sim \sum_s A_o D_{11s}^2 D_{12} D_{21} (R R_o)^{-1/2} \omega_{2+}$$

$$e^{jK_o(R+R_o) + 2jK_1 a \cos\theta_C + j\nu_s \omega_{2+} - j\pi/2} \qquad r \geq a \quad 0 \leq (\emptyset) \leq 2\pi \quad (3.3.10)$$

where $D_{12} = (N^2 - 1)^{-1/2}$, $D_{21} = 2$,

when (3.3.10) is compared to (2.3.2), determined by the ray method.

By a similar procedure for the case of m=2 there results:

$$U_3(r,\emptyset) \sim \sum_s A_o D_{11s}^2 D_{12} D_{21} (R R_o)^{-1/2} \left[R_{22} \omega_{3+} + D_{12} D_{21} \frac{\omega_{3+}^2}{2!} \right]$$

$$e^{jK_o(R+R_o) + j 4K_1 a \cos\theta_C + j\nu_s \omega_{3+} - j\pi/2} \qquad r \geq a \quad 0 \leq (\emptyset) \leq 2\pi \quad (3.3.11)$$

where $R_{22} = 1$ by comparison to the ray solution.

3.4 Conclusions

The equation for the fields developed by the ray method have thus been verified by comparison with the leading term of the asymptotic expansion of the exact solution. Also the diffraction coefficients obtained in the ray solution have been evaluated by comparison with the exact solution. The extreme case corresponding to R_{22}=1 may be explained by employing two rays, where one is completely refracted, and the other completely reflected at an internal surface of the cylinder.

CHAPTER IV

DISCUSSION OF THE RESULTS AND CONCLUSIONS

4.1 General

The asymptotic solution for the scattering and diffraction of a cylindrical wave by a dielectric cylinder, was developed in Chapter II using the geometrical theory of diffraction. The solution was obtained by constructing a few ray paths and determining the amplitude and phase relations of the ray as it travelled along the path. At an observation point, the field was simply the vector sum of the fields on all the rays passing through that point. In this problem, caustics were generated and the calculation of the field on the rays passing through these caustics was carried out following the method developed by Keller[2,10].

The two main advantages in using the ray method are:

(a) Simple computation of the scattered field which is due to the fact that an asymptotic series is inherently more rapidly convergent than the corresponding series in the exact solution.

(b) The agreement with experiment and the simple interpretation of the solution with reference to physical behaviour which may be obtained by retaining the first few terms of the asymptotic series.

The first reason was amply demonstrated when the ray solution was compared with the laborous mathematical manipulations required to determine the exact solution for the same problem, as shown in Chapter III. The fields determined by the ray method were found to be leading terms of the asymptotic expansion of the exact solution. The second reason will be shown in this Chapter.

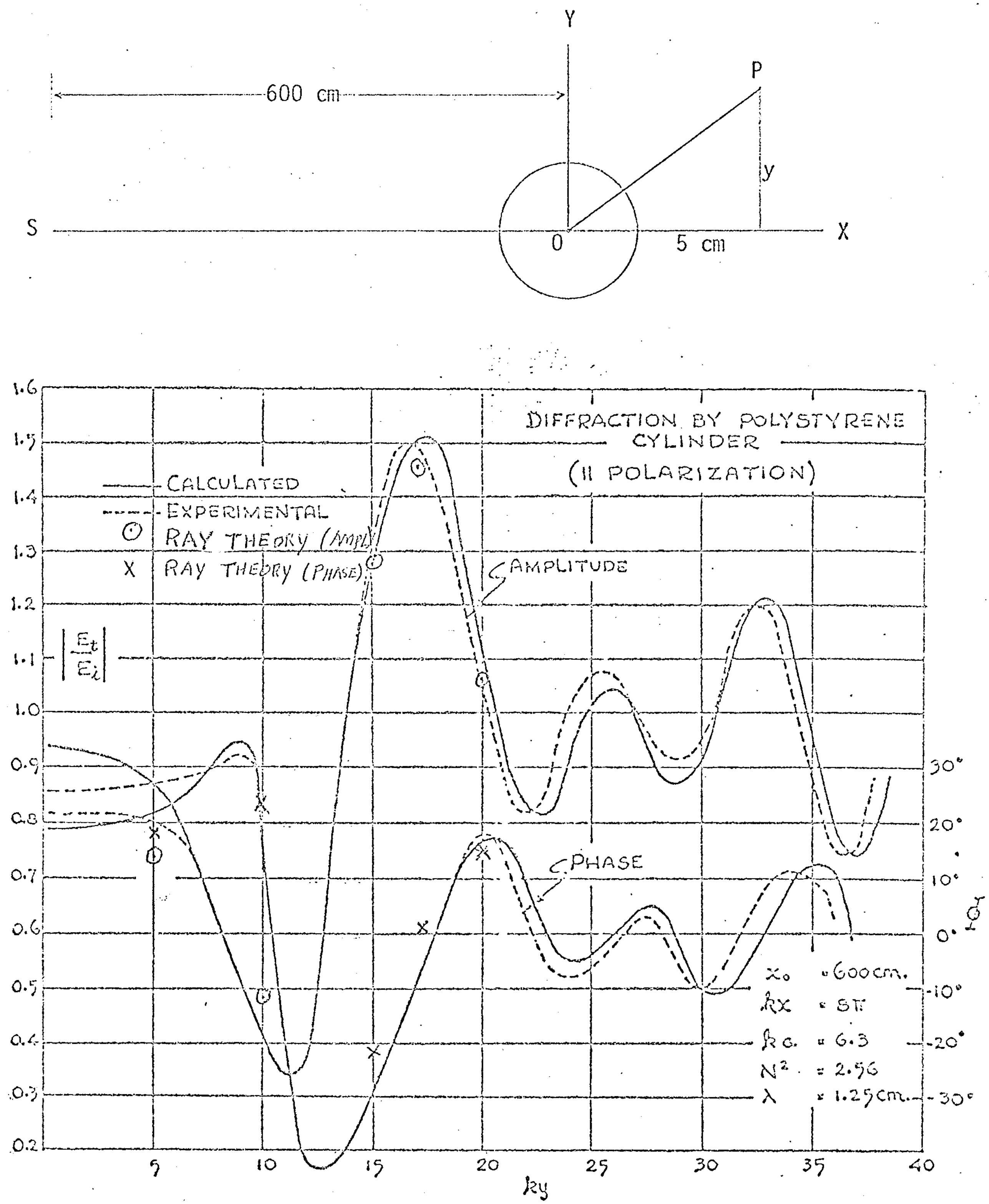

FIGURE (4.2.1)

TOTAL FIELD TO INCIDENT FIELD RATIO FOR

A POLYSTYENE CYLINDER

4.2 Comparison with Experimental and Exact Results

Fig. (4.2.1) shows the experimental results of Kodis[18] for a polystyrene cylinder having a diameter of 1 inch or 2.03λ at 24 Gcs. The exact solution, based on the theory of Froese and Wait[17] is also shown.

The results based on the ray method for the same cylinder geometry, and location of the source ond observation point, are also shown for the sake of comparison. These results are based on equation (2.2.5) for the field due to the incident ray, (2.2.8) for the reflected ray field, (2.2.13), for the first and third transmitted ray fields. A sample calculation for the field due to the various rays and showing the graphical procedure used to determine the geometry of each path, is given in Appendix (A4.1).

The agreement with experiment and the exact solution is good, and the maximum error for the amplitude and phase are 8% and 6^{o}, respectively. The error in the amplitude and phase due to the graphical procedure used to find the ray paths (Appendix A4.1) is estimated to be $\pm 2\%$ and $\pm 3^{o}$ respectively. The errors due to the uncertainty in neglecting the contribution from the higher order rays, are of the order of 0.5% and $\pm 1^{o}$, respectively.

4.3 Physical Interpretation of the Solution

An important feature of the ray method is that by considering the first order (leading term) rays, a physical insight into the behaviour of the field, is gained. The incident, reflected, diffracted and refracted rays are shown in Fig. (4.3.1).

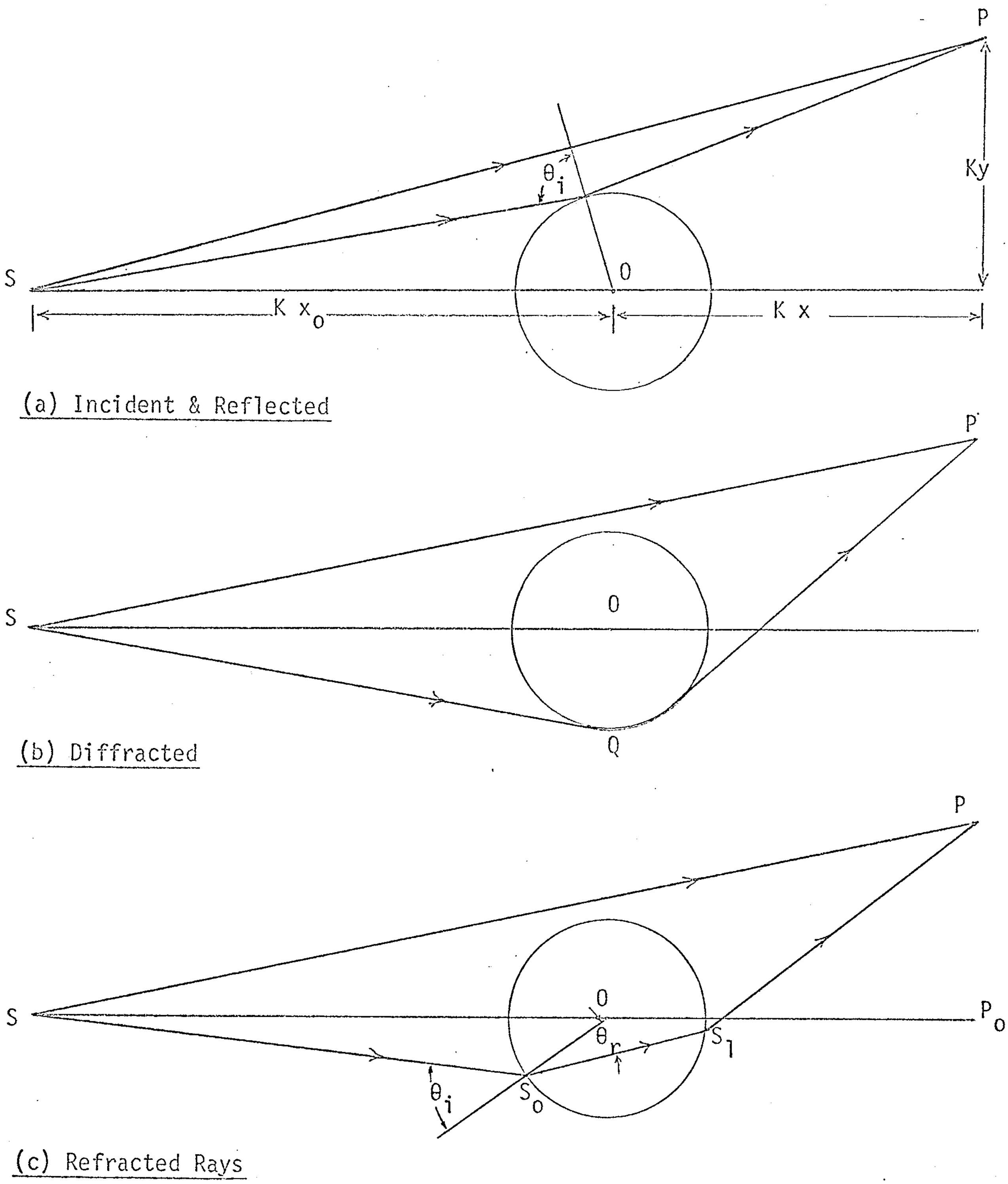

FIGURE (4.3.1)

FIRST ORDER RAYS

Examination of the relative values of Ky and $K(x + x_0)$ in Fig. (4.2.1) shows that the incident field varies very slowly in the range $0<Ky<40$, i.e.:

$$U_i = E_i \sim \frac{A_0 \, e^{jKR_i}}{\sqrt{R_i}} = \frac{A_0 \, e^{jK\sqrt{(x+x_0)^2 + y^2}}}{\sqrt{(x+x_0)^2 + y^2}}$$

$$\sim \frac{A_0}{\sqrt{(x+x_0)^2 + y^2}} \, e^{jK(x+x_0)} \, e^{\frac{jK\,y^2}{2(x+x_0)}} \qquad (4.3.1)$$

Because x_0 is very large, the ratio $y^2/2\,(x+x_0)$ is numerically small.

The reflected field U_r is zero in the shadow region (Table 2.2.1). This field is given by (2.2.8) for Ky>Ka and increases in amplitude as y increases. The reflection coefficient R_{11} is small for N small, and for a given field point, the reflected field decreases as the cylinder radius increases.

The magnitude of the diffracted field is controlled by the diffraction coefficient D_{11s} . Equation (3.3.8) shows D_{11s} is inversely proportional to large powers of Ka and N, and thus, the excited surface rays are numerically very small.

Except for Ky>>Ka, the dominant term in E_t is due to the first refracted ray. For Ky=0, the ratio (E_t/E_i) is less than unity due to the small reflection losses. The phase term of this ratio, however, is proportional to 2Ka(N-1) which indicates resonance and antiresonant regions whenever 2Ka(N-1) is an even or odd produce of π radians respectively. Thus the phase rather than the amplitude term, is very sensitive to the values of Ka and N.

For 0<Ky<Ka, the reflection losses increase while the path length SS_0S_1P is only slightly different from the incident ray path, SP, par-

ticularly for small values of Ka. Thus the amplitude ratio decreases as Ky increases while the phase term remains practically constant as shown in Fig. (4.2.1). The constant phase region increases as Ka increases and N decreases, resulting in a narrower axial beam, or focusing in the forward region.

At Ky = Ka, one incident ray excites reflected, refracted and diffracted rays at the tangency point, Q. The contribution from the diffracted and reflected rays is negligible compared to the refracted rays.

Thus the oscillations in the amplitude and phase terms in the region Ky>Ka are due to the refracted ray field and occur whenever the phase term changes by π radians, i.e.,

$$K|S\,S_0 + N(S_0S_1) + S_1P - S\,P| = t\pi\ ,\ t = 0,1,2... \qquad (4.3.2)$$

As Ky increases, the variation in (4.3.2) increases and the period of oscillation increases for this region.

For Ky>>Ka, the amplitude of the reflected ray becomes of the order of that of the refracted ray, but the two are out of phase by about π radians. The field thus oscillates about the value of the incident field and the oscillations decrease as Ky increases. The values of Ka and N have little effect on the field in this region.

4.4 Conclusions

The ray method has thus been found acceptable for determining the field, not only in the back scattering region, as was shown by Kouyoumjian[9] but also for the more general case of a field point located anywhere around the dielectric cylinder.

The ray method has also been found adequate for interpreting the oscillations in the scattering pattern, and the dependence of the field on the diameter and dielectric constant of the cylinder, as well as on the location of the source and observation point.

APPENDICES

APPENDIX (A2.1)

DERIVATION OF EQUATION (2.1.6)

The distance C_r at which two neighboring rays converge, is found by Kouyoumjian by considering the geometry of Fig. (A2.1)[9]. For a small $\Delta\alpha$,

$$R_r \frac{\Delta\theta_i - \Delta\alpha}{\cos\theta_i} = C_r \frac{\Delta\theta_i + \Delta\alpha}{\cos\theta_i} = a\ \Delta\alpha \qquad \text{(A2.1.1)}$$

By eliminating $\Delta\alpha$ there results

$$\frac{1}{C_r} = \frac{2}{a\cos\theta_i} + \frac{1}{R_r} \qquad \text{(A2.1.2)}$$

which is the Mirror Law of Optics for a convex reflector, equation (2.2.7).

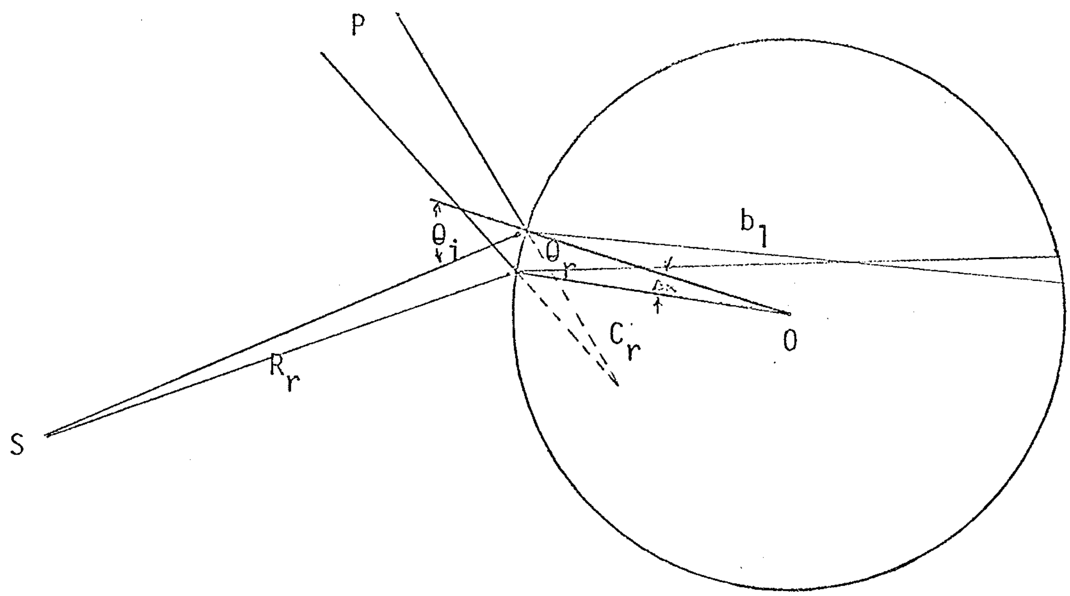

FIGURE (A2.1)

REFLECTED AND REFRACTED RAYS

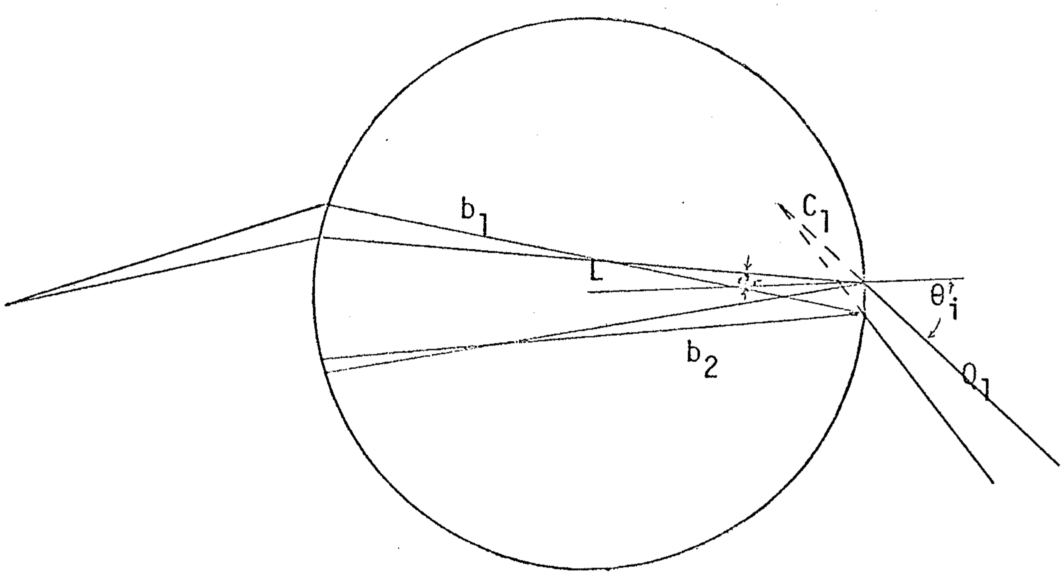

FIGURE (A2.2)

INTERNALLY REFLECTED AND REFRACTED RAYS

APPENDIX (A2.2)

DERIVATION OF EQUATION (2.1.10)

The distance b, at which two neighboring refracted rays converge in passing through the dielectric cylinder, is found by considering the geometry of Fig. (A.1.1)[9]. For small $\Delta\alpha$

$$R_r \frac{\Delta\theta - \Delta\alpha}{\cos\theta_i} = b_1 \frac{\Delta\alpha - \Delta\theta_r}{\cos\theta_r} = a\,\Delta\alpha \qquad \text{(A2.2.1)}$$

Eliminating $\Delta\alpha$ and taking limits gives:

$$\frac{1}{b_1} = \frac{1 - \frac{d\theta_r}{d\theta_i}}{a\cos\theta_r} - \frac{\cos\theta_i \frac{d\theta_r}{d\theta_i}}{R_r\cos\theta_r} \qquad \text{(A2.2.2)}$$

Snell's Law

$$\sin\theta_i = N\sin\theta_r$$

Taking derivations

$$\cos\theta_i\, d\,\theta_i = N\cos\theta_r\, d\,\theta_2$$

$$\frac{d\theta_2}{d\theta_i} = \frac{\cos\theta_i}{N\cos\theta_r} \qquad \text{(A2.2.3)}$$

$$\therefore \qquad \frac{1}{b_1} = \frac{1}{a\cos\theta_r}\left[1 - \frac{\cos\theta_i}{N\cos\theta_r} - \frac{a\cos^2\theta_i}{N R_1\cos\theta_r}\right] \qquad \text{(A2.2.4)}$$

By the mirror law of optics for a concave reflector,

$$\frac{1}{b_i} = \frac{2}{a\cos\theta_2} - \frac{1}{L - b_{i-1}} \qquad i = 2,3\ \ldots$$

given by (2.2.16).

APPENDIX (A2.3)

DERIVATION OF EQUATION (2.1.11)

Two neighboring rays, which are refracted out of the cylinder, meet when extended. The distance C from the cylinder surface along the ray extension, is found by considering the geometry of Fig. (A2.2). For small $\Delta\alpha$,

$$(L - b_1)\frac{\Delta\theta_r + \Delta\alpha}{\cos\theta_r} = C_1 \frac{\Delta\theta_i + \Delta\alpha}{\cos\theta_i} = a\,\Delta\alpha \qquad \text{(A2.3.1)}$$

Eliminating $\Delta\alpha$ and taking limits gives:

$$\frac{1}{C_1} = \frac{\cos\theta_r}{\cos\theta_i}\left[\frac{\dfrac{d\,\theta_i}{d\,\theta_r}}{L - b_1} - \frac{\dfrac{d\,\theta_i}{d\,\theta_r}}{a\cos\theta_r} + \frac{1}{a\cos\theta_r}\right]$$

$$\therefore \quad \frac{1}{C_i} = \frac{\cos\theta_r}{\cos\theta_i}\left[\frac{N\cos\theta_r}{(L - b_i)\cos\theta_i} - \frac{N}{\cos\theta_i} + \frac{1}{a\cos\theta_r}\right]$$

$$i = 1,2,3\ \ldots \qquad \text{(A2.3.2)}$$

which is equation (2.2.17).

APPENDIX (A3.1)

DERIVATION OF EQUATION (3.1.6)

Goertzel and Tralli[13] give the particular solution for radiation by an infinitely long cylinder as being:

$$U = \frac{j}{4} \sum_{\nu} e^{j\nu\emptyset} \; J_\nu (K_o r_o) \, H_\nu^{(1)}(K_o r), r>r_o \tag{A3.1.1}$$

$$= \frac{j}{4} \sum_{\nu} e^{j\nu\emptyset} \; J_\nu (K_o r) \; H_\nu^{(1)}(K_o r_o), r<r_o \tag{A3.1.2}$$

The solution of the homogeneous equation is:

$$U = +\frac{j}{4} \sum_{\nu} e^{j\nu\emptyset} \; A_n \, H_\nu^{(1)}(K_o r), \; r>r_o \tag{A3.1.3}$$

$$= +\frac{j}{4} \sum_{\nu} e^{j\nu\emptyset} \; B_n \, H_\nu^{(1)}(K_o r), \; r<r_o \tag{A3.1.4}$$

Inside the dielectric cylinder

$$U = \frac{j}{4} \sum_{\nu} e^{j\nu\emptyset} \, C_n \, J_\nu \, (K_1 r), \; r\leq a \tag{A3.1.5}$$

At a distance from the cylinder, the field sees only the line source

$\therefore \; A_n = 0$

The general solution in the region $a<r<r_o$ is:

$$U = \frac{j}{4} \sum_{\nu} e^{j\nu\emptyset} \left[J_\nu (K_o r) \, H_\nu^{(1)}(K_o r_o) + B_n \, H_\nu^{(1)}(K_o r) \right] \tag{A3.1.6}$$

For $r<a$,

$$U = \frac{j}{4} \sum_{\nu} e^{j\nu\emptyset} \; C_n \, J_\nu(K_1 r) \tag{A3.1.7}$$

Applying the boundary conditions at $r= a$

$$U(a^+, \emptyset) = U(a^-, \emptyset) \tag{A3.1.8}$$

$$J_\nu(K_o a)\, H_\nu^{(1)}(K_o r_o) + B_n\, H_\nu^{(1)}(K_o a) = C_n\, J_\nu(K_1 a)$$

$$\frac{\partial u}{\partial r}(a^+,\emptyset) = \frac{\partial u}{\partial r}(a^-,\emptyset) \qquad \text{(A3.1.9)}$$

$$K_o\left[J'_\nu(K_o a)\, H_\nu^{(1)}(K_o r_o) + B_n\, H_\nu^{(1)}(K_o a)\right] = K_1\, C_n\, J'_\nu(K_1 a)$$

Eliminating C_n these results:

$$B_n = -\left[\frac{J_\nu(K_1 a)\, J'_\nu(K_o a) - N\, J_\nu(K_o a)\, J'_\nu(K_1 a)}{J_\nu(K_1 a)\, H_\nu^{(1)}(K_o a) - N\, J'_\nu(K_1 a)\, H_\nu^{(1)}(K_o a)}\right] H_\nu^{(1)}(K_o r_o) \qquad \text{(A3.1.10)}$$

$$= -\, P_\nu\, H_\nu^{(1)}(K_o r_o) \qquad \text{(A3.1.11)}$$

as in Equation (3.1.7) where, in this region, $H_\nu^{(1)}(K_o r_o) = H_\nu^{(1)}(K_o r_>)$.

APPENDIX (A3.2)

DERIVATION OF EQUATION (3.1.9)

The expansion of the equation,

$$P_\nu = \frac{J_\nu(K_1a)\, J_\nu^{(1)'}(K_0a) - N\, J_\nu'(K_1a)\, J_\nu(K_0a)}{J_\nu'(K_1a)\, H_\nu^{(1)'}(K_0a) - N\, J_\nu'(K_1a)\, H_\nu^{(1)}(K_0a)} \tag{A3.2.1}$$

is carried out using the identities,

$$J_\nu(z) = \frac{1}{2}\left[H_{\nu}^{(1)}(z) + H_\nu^{2}(z)\right] \tag{A3.2.2}$$

$$J_\nu'(z) = \frac{1}{2}\left[H_\nu^{(1)'}(z) + H_\nu^{2'}(z)\right] \tag{A3.2.3}$$

Using (A3.2.2) and (A3.2.3) in (A3.2.1) and multiplying,

$$P_\nu = \frac{1}{2}\left[\frac{H_\nu^{(1)}(K_1a)\, H_\nu^{(1)'}(K_0a) + H_\nu^{(2)}(K_1a)\, H_\nu^{(1)'}(K_0a) - N\left(H_\nu^{(1)}(K_0a)\, H_\nu^{(1)'}(K_1a) + H_\nu^{(1)}(K_0a)\, H_\nu^{(2)'}(K_1a)\right)}{H_\nu^{(1)}(K_1a)\, H_\nu^{(1)'}(K_0a) + H_\nu^{(2)}(K_1a)\, H_\nu^{(1)'}(K_0a) - N\left(H_\nu^{(1)}(K_0a)\, H_\nu^{(1)'}(K_1a) + H_\nu^{(1)}(K_0a)\, H_\nu^{(2)'}(K_1a)\right)}\right.$$

$$\left.\times\ \frac{H_\nu^{(1)}(K_1a)\, H_\nu^{(2)'}(K_0a) + H_\nu^{(2)}(K_1a)\, H_\nu^{2'}(K_0a) - N\left(H_\nu^{(2)}(K_1a)\, H_\nu^{(1)'}(K_1a) + H_\nu^{(2)}(K_1a)\, H_\nu^{(2)'}(K_1a)\right)}{H_\nu^{(1)}(K_1a)\, H_\nu^{(1)'}(K_0a) + H_\nu^{(2)}(K_1a)\, H_\nu^{(1)'}(K_0a) - N\left(H_\nu^{(1)}(K_0a)\, H_\nu^{(1)'}(K_1a) + H_\nu^{(1)}(K_0a)\, H_\nu^{(2)'}(K_1a)\right)}\right]$$

$$\approx \frac{1}{2}\left[1 + \frac{H_\nu^{(2)}(K_0a)}{H_\nu^{(1)}(K_0a)}\left\{\frac{\dfrac{H_\nu^{(1)}(K_1a)\, H_\nu^{(2)'}(K_0a)}{H_\nu^{(2)}(K_1a)\, H_\nu^{(2)}(K_0a)} + \dfrac{H_\nu^{(2)'}(K_0a)}{H_\nu^{(2)}(K_0a)} - N\dfrac{H_\nu^{(1)'}(K_1a)}{H_\nu^{(2)}(K_1a)} - N\dfrac{H_\nu^{(2)'}(K_1a)}{H_\nu^{(2)}(K_1a)}}{\dfrac{H_\nu^{(1)}(K_1a)\, H_\nu^{(1)'}(K_0a)}{H_\nu^{(2)}(K_1a)\, H_\nu^{(1)}(K_0a)} + \dfrac{H_\nu^{(1)'}(K_0a)}{H_\nu^{(1)}(K_0a)} - N\dfrac{H_\nu^{(1)'}(K_1a)}{H_\nu^{(2)}(K_1a)} - N\dfrac{H_\nu^{(2)'}(K_1a)}{H_\nu^{(2)}(K_1a)}}\right\}\right] \tag{A3.2.4}$$

Dividing through by L where:

$$L = \frac{H_\nu^{(1)'}(K_0a)}{H_\nu^{(1)}(K_0a)} - N\,\frac{H_\nu^{(2)'}(K_1a)}{H_\nu^{(2)}(K_1a)} \tag{A3.2.5}$$

$$P_\nu = \frac{1}{2}\left[1 - \frac{H_\nu^{(2)}(K_0a)}{H_\nu^{(1)}(K_0a)}\left\{\frac{R_{11} - \frac{\frac{H_\nu^{(1)}(K_1a)\,H_\nu^{(2)'}(K_0a)}{H_\nu^{(2)}(K_1a)\,H_\nu^{(1)}(K_0a)} + N\frac{H_\nu^{(1)'}(K_1a)}{H_\nu^{(2)}(K_1a)}}{L}}{1 - \frac{H_\nu^{(1)}(K_1a)}{H_\nu^{(2)}(K_1a)}R_{22}}\right\}\right] \qquad \text{(A3.2.6)}$$

Expanding the denominator in a binomial series,

$$P_\nu = \frac{1}{2}\left[1 - \frac{H_\nu^{(2)}(K_0a)}{H_\nu^{(1)}(K_0a)}\left\{R_{11} + R_{11}R_{22}\sum_{m=1}^{\infty}\left(\frac{H_\nu^{(1)}(K_1a)}{H_\nu^{(2)}(K_1a)}\right)^m R_{22}^{m-1}\right.\right.$$

$$\left.\left. + \frac{H_\nu^{(1)}(K_1a)}{H_\nu^{(2)}(K_1a)}\left(\frac{-\frac{H_\nu^{(2)'}(K_0a)}{H_\nu^{(2)}(K_0a)} + N\frac{H_\nu^{(1)'}(K_1a)}{H_\nu^{(1)}(K_1a)}}{L}\right)\sum_{m=0}^{\infty}\left(\frac{H_\nu^{(1)}(K_1a)}{H_\nu^{(2)}(K_1a)}R_{22}\right)^m\right\}\right]$$

$$= \frac{1}{2}\left[1 - \frac{H_\nu^{(2)}(K_0a)}{H_\nu^{(1)}(K_0a)}\left\{R_{11} + \left(R_{11}R_{22} - \frac{\frac{H_\nu^{(1)'}(K_0a)}{H_\nu^{(1)}(K_0a)} + N\frac{H_\nu^{(1)'}(K_1a)}{H_\nu^{(1)}(K_1a)} - \frac{H_\nu^{(2)'}(K_0a)}{H_\nu^{(2)}(K_0a)}}{L}\right.\right.\right.$$

$$\left.\left.\left. + \frac{+N\frac{H_\nu^{(2)'}(K_1a)}{H_\nu^{(2)}(K_1a)} + \frac{H_\nu^{(1)'}(K_0a)}{H_\nu^{(1)}(K_0a)} - N\frac{H_\nu^{(2)'}(K_1a)}{H_\nu^{(2)}(K_1a)}}{L}\right)\sum_{m=1}^{\infty}\left(\frac{H_\nu^{(1)}(K_1a)}{H_\nu^{(2)}(K_1a)}\right)^m R_{22}^{m-1}\right\}\right]$$

$$= \frac{1}{2}\left[1 - \frac{H_\nu^{(2)}(K_0a)}{H_\nu^{(1)}(K_0a)}\left\{R_{11} + \left(R_{11}R_{22} + R_{22} + R_{11} + 1\right)\sum_{m=1}^{\infty}\left(\frac{H_\nu^{(1)}(K_1a)}{H_\nu^{(2)}(K_1a)}\right)^m R_{22}^{m-1}\right\}\right]$$

$$= \frac{1}{2}\left[1 - \frac{H_\nu^{(2)}(K_0a)}{H_\nu^{(1)}(K_0a)}\left\{R_{11} + T_{12}T_{21}\sum_{m=1}^{\infty}\left(\frac{H_\nu^{(1)}(K_1a)}{H_\nu^{(2)}(K_1a)}\right)^m R_{22}^{m-1}\right\}\right] \qquad \text{(A2.3.7)}$$

which is the expansion given by (3.1.9).

APPENDIX (A3.3)

ASYMPTOTIC FORMS OF HANKEL FUNCTION

Debye asymptotic forms[15] for large argument and index, with $\nu < z$ are:

$$H_\nu^{(1)}(z) \sim \left(\frac{1}{2}\pi z \sin\tau\right)^{-1/2} e^{jz(\sin\tau - \tau\cos\tau) - j\pi/4} \equiv F(z)$$

$$H_\nu^{(2)}(z) \sim \left(\frac{1}{2}\pi z \sin\tau\right)^{-1/2} e^{-jz(\sin\tau - \tau\cos\tau) + j\pi/4} \equiv G(z)$$

$$\frac{\partial}{\partial z} H_\nu^{(1)}(z) \sim j \sin\tau \, F(z)$$

$$\frac{\partial}{\partial z} H_\nu^{(2)}(z) \sim -j \sin\tau \, G(z)$$

where $\tau = \cos^{-1}\frac{\nu}{z}$.

For argument and index both large, and $\nu \simeq z$, the Airy function representations for the Hankel functions are:

$$H_\nu^{(1)}(z) \sim \left(\frac{2}{\pi}\right) y \, A(g)$$

$$H_\nu^{(2)}(z) \sim \left(\frac{2}{\pi}\right) x \, A(t)$$

$$H_\nu^{(1)'}(z) \quad \left(\frac{2}{\pi}\right) y^2 A'(g)$$

$$H_\nu^{(2)'}(z) \sim -\left(\frac{2}{\pi}\right) x^2 A'(t)$$

$$\frac{\partial}{\partial \nu} H_\nu^{(1)}(z) \sim \left(\frac{2}{\pi}\right) y^2 A'(g)$$

$$\frac{\partial}{\partial \nu} H_\nu^{(2)}(z) \sim \left(\frac{2}{\pi}\right) x^2 A'(t)$$

$$\frac{\partial}{\partial \nu} H_\nu^{(1)'}(z) \sim \left(\frac{2}{\pi}\right) \left(\frac{y^3}{3}\right) g A(g)$$

and $\frac{\partial}{\partial \nu} H_{\nu}^{(2)'}(z) \sim (\frac{2}{\pi}) (\frac{x^3}{3}) t A(t)$

where $y = (\frac{6}{z})^{1/3} \; e^{-j\pi/3}$

$$x = (\frac{6}{z})^{1/3} \; e^{j\pi/3}$$

$$g = y \, (\nu - z)$$

$$t = x \, (\nu - z)$$

APPENDIX (A3.4)

SADDLE POINT EVALUATION OF EQUATION (3.2.1)

$$U_i(r,\phi) = \frac{i}{8}\sum_{n=-\infty}^{\infty}\left[\int_{-\infty}^{\infty} e^{i\nu(\phi+2\pi n)} H_\nu^{(1)}(k_0 r_>)\, H_\nu^{(1)}(k_0 r_<)\, d\nu \right.$$

$$\left. + \int_{-\infty}^{\infty} e^{i\nu(\phi+2\pi n)} H_\nu^{(1)}(k_0 r_>)\, H_\nu^{(2)}(k_0 r_<)\, d\nu\right] \quad r \geq a \quad 0<\phi<2\pi$$

$$0 < |\phi| < 2\pi \quad \text{(A3.4.1)}$$

Substituting the Debye asymptotic forms:

$$U_i \sim \frac{i}{8}\sum_{n=-\infty}^{\infty}\left[\int_{-\infty}^{\infty} e^{i\nu(\phi+2\pi n)} \frac{e^{ik_0 r_>\left[\sin\left(\cos^{-1}\frac{\nu}{k_0 r_>}\right) - \frac{\nu}{k_0 r_>}\cos^{-1}\frac{\nu}{k_0 r_>}\right] - i\pi/4}}{\left[\frac{\pi}{2} k_0 r_> \sin\left(\cos^{-1}\frac{\nu}{k_0 r_>}\right)\right]^{1/2}\left[\frac{\pi}{2} k_0 r_< \sin\left(\cos^{-1}\frac{\nu}{k_0 r_<}\right)\right]^{1/2}}\right.$$

$$\times e^{ik_0 r_<\left[\sin\left(\cos^{-1}\frac{\nu}{k_0 r_<}\right) - \frac{\nu}{k_0 r_<}\cos^{-1}\frac{\nu}{k_0 r_<}\right] - i\pi/4}\, d\nu + \int_{-\infty}^{\infty} e^{i\nu(\phi+2\pi n)}\, d\nu$$

$$\left.\times \frac{e^{ik_0 r_>\left[\sin\left(\cos^{-1}\frac{\nu}{k_0 r_>}\right) - \frac{\nu}{k_0 r_>}\cos^{-1}\frac{\nu}{k_0 r_>}\right] - i\pi/4}\; e^{-ik_0 r_<\left[\sin\cos^{-1}\frac{\nu}{k_0 r_<} - \frac{\nu}{k_0 r_<}\cos^{-1}\frac{\nu}{k_0 r_<}\right] + i\pi/4}}{\left[\frac{\pi}{2} k_0 r_> \sin\left(\cos^{-1}\frac{\nu}{k_0 r_>}\right)\right]^{1/2}\left[\frac{\pi}{2} k_0 r_< \sin\left(\cos^{-1}\frac{\nu}{k_0 r_<}\right)\right]^{1/2}}\right]$$

$$\sim \frac{i}{8}\sum_{n=-\infty}^{\infty}\left[\int_{-\infty}^{\infty} e^{i\nu(\phi+2\pi n)} \frac{e^{i\left[\sqrt{(k_0 r_>)^2-\nu^2} - \nu\cos^{-1}\frac{\nu}{k_0 r_>}\right] + i\left[\sqrt{(k_0 r_<)^2-\nu^2} - \nu\cos^{-1}\frac{\nu}{k_0 r_<}\right]}}{\frac{\pi}{2}\left[\left((k_0 r_>)^2-\nu^2\right)\left((k_0 r_<)^2-\nu^2\right)\right]^{1/4}}\, d\nu\right.$$

$$\left. + \int_{-\infty}^{\infty} e^{i\nu(\phi+2\pi n)} \frac{e^{i\left[\sqrt{(k_0 r_>)^2-\nu^2} - \nu\cos^{-1}\frac{\nu}{k_0 r_>}\right] - i\left[\sqrt{(k_0 r_<)^2-\nu^2} - \nu\cos^{-1}\frac{\nu}{k_0 r_<}\right]}}{\frac{\pi}{2}\left[\left((k_0 r_>)^2-\nu^2\right)\left((k_0 r_<)^2-\nu^2\right)\right]^{1/4}}\, d\nu\right]$$

$$\sim I_1 + I_2 \quad \text{(A3.4.2)}$$

By the Saddle Point method,

$$I(z) = \int_c X(z)\, e^{t f(z)}\, dz \sim \sqrt{\frac{2\pi}{t}}\, \frac{X(z_0)\, e^{t f(z_0)}}{\left[-f''(z_0)\right]^{1/2}} \tag{A3.4.3}$$

The phase term of I_1 =

$$\nu(\phi + 2\pi n) + \sqrt{(K_0 r_>)^2 - \nu^2} - \nu \cos^{-1}\frac{\nu}{K_0 r_>} - \frac{i\pi}{2} + \sqrt{(K_0 r_<)^2 - \nu^2}$$
$$- \nu \cos^{-1}\frac{\nu}{K_0 r_<} \tag{A3.4.4}$$

At the Saddle Point, $\frac{\partial}{\partial \nu}(\text{PHASE}) = 0$ or

$$\phi + 2\pi n = \cos^{-1}\frac{\nu_0}{K_0 r_>} + \cos^{-1}\frac{\nu_0}{K_0 r_<} \tag{A3.4.5}$$

which for a real saddle point is the same as (3.2.2). By evaluating (A3.4.4) at the saddle point, there results,

$$I_1 \sim \frac{i}{8}\sqrt{\frac{2\pi}{i}}\, \frac{e^{i\left[\sqrt{(K_0 r_>)^2 - \nu_0^2} + \sqrt{(K_0 r_<)^2 - \nu_0^2}\right] - \frac{i\pi}{2}}}{\frac{\pi}{2}\left[\sqrt{(K_0 r_>)^2 - \nu^2}\sqrt{(K_0 r_<)^2 - \nu^2}\right]^{1/2}\left[-\frac{1}{\sqrt{(K_0 r_>)^2 - \nu^2}} - \frac{1}{\sqrt{(K_0 r_<)^2 - \nu^2}}\right]^{1/2}}$$

$$\sim \sqrt{\frac{i}{8\pi K_0}}\, \frac{e^{-i\pi/2}\, e^{iK_0\left[\sqrt{r_>^2 - \left(\frac{\nu_0}{K_0}\right)^2} + \sqrt{r_<^2 - \left(\frac{\nu_0}{K_0}\right)^2}\right]}}{i\left[\sqrt{r_>^2 - \left(\frac{\nu_0}{K_0}\right)^2} + \sqrt{r_<^2 - \left(\frac{\nu_0}{K_0}\right)^2}\right]^{1/2}}$$

$$\sim \frac{A_0\, e^{iK_0 R_i}}{\sqrt{R_i}} \tag{A3.4.6}$$

Similarly,

$$I_2 \sim \sqrt{\frac{i}{8\pi K_0}}\, \frac{e^{iK_0\left[\sqrt{r_>^2 - \left(\frac{\nu_0}{K_0}\right)^2} - \sqrt{r_<^2 - \left(\frac{\nu_0}{K_0}\right)^2}\right]}}{\left[\sqrt{r_>^2 - \left(\frac{\nu_0}{K_0}\right)^2} - \sqrt{r_<^2 - \left(\frac{\nu_0}{K_0}\right)^2}\right]^{1/2}} \sim \frac{A_0\, e^{iK_0 R_i}}{\sqrt{R_i}} \tag{A3.4.7}$$

Outside and inside the shaded area respectively, (A3.4.6) and (A3.4.7) are identical to (3.2.4).

APPENDIX (A3.5)

SADDLE POINT EVALUATION OF REFLECTED FIELD, EQUATION (3.2.5)

$$U_r(r,\phi) \sim \frac{j}{8}\sum_{n=-\infty}^{\infty}\int_{-\infty}^{\infty} e^{j\nu(\phi+2\pi n)} R_{ii}\; H_\nu^{(2)}(k_0a)\, H_\nu^{(1)}(k_0r_>)\, H_\nu^{(1)}(k_0r_<)\, d\nu \quad \text{(A3.5.1)}$$

$$r \geq a \qquad 0 < |\phi| < 2\pi$$

Expand R_{11} and apply the Debye asymptotic forms:

$$R_{ii} = -\frac{-j\sin\cos^{-1}\frac{\nu}{k_0a} + Nj\sin\cos^{-1}\frac{\nu}{k_1a}}{j\sin\cos^{-1}\frac{\nu}{k_0a} + Nj\sin\cos^{-1}\frac{\nu}{k_1a}}$$

$$= -\frac{\frac{\sqrt{(k_0a)^2-\nu^2}}{k_0a} + N\frac{\sqrt{(k_1a)^2-\nu^2}}{k_1a}}{\frac{\sqrt{(k_0a)^2-\nu^2}}{k_0a} + N\frac{\sqrt{(k_1a)^2-\nu^2}}{k_1a}}$$

Substitute: $\nu = \pm k_0a\sin\theta_i$;

$$R_{ii} = \frac{\cos\theta_i - N\cos\theta_r}{\cos\theta_i + N\cos\theta_r} \quad \text{(A3.5.2)}$$

The coefficients thus make no contribution to the asympototic expansion of the integrand.

$$U_r(r,\phi) \sim \frac{j}{8}\sum_{n=-\infty}^{\infty}\int_{-\infty}^{\infty} e^{j\nu(\phi+2\pi n)} R_{ii} \frac{\left(\frac{\pi}{2}k_0a\sin\cos^{-1}\right)^{-1/2} e^{-jk_0a\left[\sin\cos^{-1}\frac{\nu}{k_0a} - \frac{\nu}{k_0a}\cos^{-1}\frac{\nu}{k_0a}\right]+j\pi/4}}{\left(\frac{\pi}{2}k_0a\sin\cos^{-1}\frac{\nu}{k_0a}\right)^{-1/2} e^{jk_0a\left[\sin\cos^{-1}\frac{\nu}{k_0a} - \frac{\nu}{k_0a}\cos^{-1}\frac{\nu}{k_0a}\right]-j\pi/4}}$$

$$\times \frac{e^{jk_0r_>\left[\sin\cos^{-1}\frac{\nu}{k_0r_>} - \frac{\nu}{k_0r_>}\cos^{-1}\frac{\nu}{k_0r_>}\right] - j\pi/4}\; e^{jk_0r_<\left[\sin\cos^{-1}\frac{\nu}{k_0r_<} - \frac{\nu}{k_0r_<}\cos^{-1}\frac{\nu}{k_0r_<}\right] - j\pi/4}}{\left(\frac{\pi}{2}k_0r_>\sin\cos^{-1}\frac{\nu}{k_0r_>}\right)^{1/2}\left(\frac{\pi}{2}k_0r_<\sin\cos^{-1}\frac{\nu}{k_0r_<}\right)^{1/2}}\, d\nu$$

$$\sim \frac{j}{8}\sum_n\int_{-\infty}^{\infty} R_{ii}\frac{e^{j\nu(\phi+2\pi n)}\, e^{-2j\left[\sqrt{(k_0a)^2-\nu^2} - \nu\cos^{-1}\frac{\nu}{k_0a}\right] + j\left[\sqrt{(k_0r_>)^2-\nu^2} - \nu\cos^{-1}\frac{\nu}{k_0r_>}\right] + j\left[\sqrt{(k_0r_<)^2-\nu^2} - \nu\cos^{-1}\frac{\nu}{k_0r_<}\right]}}{\frac{\pi}{2}\left(\sqrt{(k_0r_>)^2-\nu^2}\right)^{1/2}\left(\sqrt{(k_0r_<)^2-\nu^2}\right)^{1/2}}\, d\nu$$

(A3.5.3)

The stationary phase point is:

$$\phi + 2\pi n = \cos^{-1}\frac{\nu_0}{k_0r_>} + \cos^{-1}\frac{\nu_0}{k_0r_<} - 2\cos^{-1}\frac{\nu}{k_0a} \quad \text{(A3.5.4)}$$

Substituting in the saddle point equation (A3.4.3):

$$U_r(r,\phi) \sim \sqrt{\frac{j}{8\pi K_0}}\;\frac{R_{11}\; e^{jK_0\left[\sqrt{(r_>)^2-\left(\frac{\nu}{K_0}\right)^2}+\sqrt{(r_<)^2-\left(\frac{\nu}{K_0}\right)^2}-2\sqrt{a^2-\left(\frac{\nu}{K_0}\right)^2}\right]}}{\left[\sqrt{r_>^2-\left(\frac{\nu}{K_0}\right)^2}\sqrt{r_<^2-\left(\frac{\nu}{K_0}\right)^2}\right]^{1/2}\left[\frac{2}{\sqrt{a^2-\left(\frac{\nu}{K_0}\right)^2}}-\frac{1}{\sqrt{r_>^2-\left(\frac{\nu}{K_0}\right)^2}}-\frac{1}{\sqrt{r_<^2-\left(\frac{\nu}{K_0}\right)^2}}\right]^{1/2}} \qquad \text{(A3.5.5)}$$

$$\sim \sqrt{\frac{j}{8\pi K_0}}\;\frac{R_{11}\; e^{jK_0\left[\sqrt{r_>^2-\left(\frac{\nu}{K_0}\right)^2}-\sqrt{a^2-\left(\frac{\nu}{K_0}\right)^2}+\sqrt{r_<^2-\left(\frac{\nu}{K_0}\right)^2}-\sqrt{a^2-\left(\frac{\nu}{K_0}\right)^2}\right]}}{\left[\frac{2\sqrt{r_>^2-\left(\frac{\nu}{K_0}\right)^2}\sqrt{r_<^2-\left(\frac{\nu}{K_0}\right)^2}}{\sqrt{a^2-\left(\frac{\nu}{K_0}\right)^2}}-2\sqrt{r_<^2-\left(\frac{\nu}{K_0}\right)^2}-2\sqrt{r_>^2-\left(\frac{\nu}{K_0}\right)^2}+2\sqrt{a^2-\left(\frac{\nu}{K_0}\right)^2}+\sqrt{r_<^2-\left(\frac{\nu}{K_0}\right)^2}+\sqrt{r_>^2-\left(\frac{\nu}{K_0}\right)^2}-2\sqrt{a^2-\left(\frac{\nu}{K_0}\right)^2}\right]^{1/2}}$$

Substituting, $\nu_i = \pm K_0 a \sin\theta_i$

$$U_r(r,\phi) \sim \sqrt{\frac{j}{8\pi K_0}}\;\frac{R_{11}\; e^{jK_0\left[\sqrt{r_>^2-a^2\sin^2\theta_i}-a\cos\theta_i+\sqrt{r_<^2-a^2\sin^2\theta_i}-a\cos\theta_i\right]}}{\left[\sqrt{r_<^2-a^2\sin^2\theta_i}-a\cos\theta_i+\left\{\left(\sqrt{r_>^2-a^2\sin^2\theta_i}-a\cos\theta_i\right)\left(\sqrt{r_<^2-a^2\sin^2\theta_i}-a\cos\theta_i\right)\right\}\times\left\{\frac{1}{\sqrt{r_<^2-a^2\sin^2\theta_i}-a\cos\theta_i}+\frac{2}{a\cos\theta_i}\right\}\right]^{1/2}}$$

$$\sim \frac{A_0\, R_{11}\, e^{jK_0(R_r+Q_r)}}{\sqrt{R_r}\left(1+\frac{Q_r}{C_r}\right)^{1/2}} \qquad \text{(A3.5.6)}$$

APPENDIX (A3.6)

EVALUATION OF THE REFRACTED FIELD, EQUATION (3.1.13)

The following equation is evaluated by the Saddle Point method:

$$U_m(r,\phi) \sim \frac{j}{8}\sum_n \int_{-\infty}^{\infty} e^{j\nu(\phi+2\pi n)}\, T_{12} T_{21} R_{22}^{m-1} H_\nu^{(1)}(K_0 r_>)\, H_\nu^{(1)}(K_0 r_<)\, \frac{H_\nu^{(2)}(K_0 a)}{H_\nu^{(1)}(K_0 a)} \left(\frac{H_\nu^{(1)}(K_1 a)}{H_\nu^{(2)}(K_1 a)}\right)^m d\nu$$

$$r \geq a \qquad 0 < |\phi| < 2\pi \qquad \text{(A3.6.1)}$$

Substituting the Debyeasymptotic forms of the Hankel function:

$$U_m(r,\phi) \sim \frac{j}{8}\sum \int_{-\infty}^{\infty} \frac{e^{j\nu(\phi+2\pi n)}\, T_{12} T_{21} R_{22}^{m-1}\, e^{-2j\left(\sqrt{(K_0 a)^2-\nu^2} - \nu\cos^{-1}\frac{\nu}{K_0 a}\right)}}{\frac{\pi}{2}\left(\sqrt{(K_0 r_>)^2-\nu^2}\right)^{1/2}\left(\sqrt{(K_0 r_<)^2-\nu^2}\right)^{1/2}}$$

$$\times\; e^{j\left(\sqrt{(K_0 r_>)^2-\nu^2} - \nu\cos^{-1}\frac{\nu}{K_0 a}\right) + j\left(\sqrt{(K_0 r_<)^2-\nu^2} - \nu\cos^{-1}\frac{\nu}{K_0 a}\right)}$$

$$\times\; e^{2mj\left(\sqrt{(K_1 a)^2-\nu^2} - \nu\cos^{-1}\frac{\nu}{K_1 a}\right) - j\frac{m\pi}{2}}\, d\nu \qquad \text{(A3.6.2)}$$

The saddle point is located at:

$$\phi + 2\pi n = -2\cos^{-1}\frac{\nu_0}{K_0 a} + \cos^{-1}\frac{\nu_0}{K_0 r_>} + \cos^{-1}\frac{\nu_0}{K_0 r_<} + 2m\cos^{-1}\frac{\nu}{K_1 a}$$

(A3.6.3)

Evaluating the integral at the saddle point:

$$U_m \sim \sqrt{\frac{j}{8\pi K_0}}\, \frac{T_{12} T_{21} R_{22}^{m-1}\, e^{-2j\sqrt{(K_0 a)^2-\nu_0^2} + j\sqrt{(K_0 r_>)^2-\nu_0^2} + j\sqrt{(K_0 r_<)^2-\nu_0^2} + 2mj\sqrt{(K_1 a)^2-\nu_0^2} - j\frac{m\pi}{2}}}{\left[\sqrt{(r_>)^2-\left(\frac{\nu_0}{K_0}\right)^2}\sqrt{r_<^2-\left(\frac{\nu_0}{K_0}\right)^2}\right]^{1/2}\left[\frac{2}{\sqrt{a^2-\left(\frac{\nu_0}{K_0}\right)^2}} - \frac{1}{\sqrt{r_>^2-\left(\frac{\nu_0}{K_0}\right)^2}} - \frac{1}{\sqrt{r_<^2-\left(\frac{\nu_0}{K_0}\right)^2}} - \frac{2m}{N\sqrt{a^2-\left(\frac{\nu}{NK_0}\right)^2}}\right]^{1/2}}$$

(A3.6.4)

Let m = 2. Multiply through the denominator, where,

$$R_2 = \sqrt{r_>^2-\left(\frac{\nu}{K_0}\right)^2} - \sqrt{a^2-\left(\frac{\nu}{K_0}\right)^2} \quad \text{and} \quad Q_2 = \sqrt{r_<^2-\left(\frac{\nu}{K_0}\right)^2} - \sqrt{a^2-\left(\frac{\nu}{K_0}\right)^2}$$

$$(\text{DENOMINATOR})^{1/2} = 2\,\frac{\left(Q_2 R_2 + R_2\sqrt{a^2-\left(\frac{\nu}{K_0}\right)^2} + Q_2\sqrt{a^2-\left(\frac{\nu}{K_0}\right)^2} + a^2-\left(\frac{\nu}{K_0}\right)^2\right)}{\sqrt{a^2-\left(\frac{\nu}{K_0}\right)^2}} - R_2 - Q_2 - 2\sqrt{a^2-\left(\frac{\nu}{K_0}\right)^2}$$

$$-4\,\frac{\left(R_2Q_2 + R_2\sqrt{a^2-\left(\frac{v}{K_0}\right)^2} + Q\sqrt{a^2-\left(\frac{v}{K_0}\right)^2} + a^2-\left(\frac{v}{K_0}\right)^2\right)}{N\sqrt{a^2-\left(\frac{v}{NK_0}\right)^2}}$$

Substitute $v_0 = \pm K_0 a \sin\theta_i$,

$$(D_{EN})^{1/2} = \frac{2NQ_2R_2\cos\theta_r + NR_2 a\cos\theta_i\cos\theta_r + NQ_2 a\cos\theta_i\cos\theta_i}{Na\cos\theta_i\cos\theta_r}$$

$$-\frac{4R_2Q_2\cos\theta_i - 4R_2 a\cos^2\theta_i - 4Qa\cos^2\theta_i - 4a^2\cos^3\theta_i}{Na\cos\theta_i\cos\theta_r}$$

$$= R_2\left[\frac{a\cos\theta_i(NR_2\cos\theta_r - 4R_2\cos\theta_i - 4a\cos^2\theta_i)}{NRa\cos\theta_i\cos\theta_r}\right.$$

$$\left.+\,Q_2\frac{(2R_2N\cos\theta_r - 4R_2\cos\theta_i - 4a\cos^2\theta_i + Na\cos\theta_r\cos\theta_i)}{NRa\cos\theta_i\cos\theta_r}\right]$$

$$= R_2\left[\frac{NR_2\cos\theta_r - 4R\cos\theta_i - 4a^2\cos^2\theta_i}{NR\cos\theta_r}\right] \times$$

$$\frac{a\cos\theta_i(NR_2\cos\theta_r - 4R_2\cos\theta_i - 4a\cos^2\theta_i) + Q_2(2R_2N\cos\theta_r - 4R_2\cos\theta_i}{a\cos\theta_i(NR_2\cos\theta_r - 4R_2\cos\theta_i - 4a\cos^2\theta_i)}$$

$$\left.\times\,\frac{-4a\cos^2\theta_i + Na\cos\theta_i\cos\theta_r)}{}\right]$$

$$= R_2\left[\frac{NR_2\cos\theta_r - 2R_2\cos\theta_i - 2a\cos^2\theta_i}{NR_2\cos\theta_r}\right]\left[\frac{NR_2\cos\theta_r - 4R_2\cos\theta_i - 4a\cos^2\theta_i}{NR_2\cos\theta_r - 2R_2\cos\theta_i - 2a\cos^2\theta_i}\right]$$

$$\times\left[1 + \frac{Q_2(2NR_2\cos\theta_r - 4R_2\cos\theta_i - 4a\cos^2\theta_i + Na\cos\theta_r\cos\theta_i)}{a\cos\theta_i(NR_2\cos\theta_r - 4R_2\cos\theta_i - 4a\cos^2\theta_i)}\right]$$

$$= R_2\left(\frac{L}{b_1} - 1\right)\left(\frac{L}{b_2} - 1\right)\left(1 + \frac{Q_2}{C_2}\right) \qquad \text{(A3.6.5)}$$

When the phase term, $e^{-i\pi}$ is taken into the denominator, then

$$U_2(y,b) \sim A_0 T_{12}T_{21} R_{22} N_1 N_2 M_2\, e^{jK_0(R_2+Q_2) + j2k_1L}$$

which is (3.1.13) with m = 2 .

APPENDIX (A3.7)

EVALUATION OF EQUATION (3.3.3) BY THE METHOD OF RESIDUES

The following equation is evaluated by the method of Residues:

$$U_r(r,\phi) \sim \frac{j}{8}\int_{-\infty}^{\infty} e^{j\nu(\phi+2\pi n)} H_\nu^{(1)}(K_0 r_>)\, H_\nu^{(1)}(K_0 r_<) \left[R_{11}\frac{H_\nu^{(2)}(K_0 a)}{H_\nu^{(1)}(K_0 a)} - 1\right] d\nu$$

$$r \geq a \qquad 0 < (\phi) < 2\pi \qquad \text{(A3.7.1)}$$

By the method of residues,

$$\int_c f(z)\, dz = 2\pi j \sum \text{residues} \qquad \text{(A3.7.2)}$$

The denominator of R_{11} determines the pole locations. Thus the second term makes no contribution to the integral. The transendental equation is evaluated at each of the poles by expanding it in a Taylor series at the pole,

$$g(z) = g(a) + (z-a)\, g'(a). \qquad \text{(A3.7.3)}$$

Thus

$$U_r(r,\phi) \sim 2\pi j \frac{j}{8} \sum_{\nu_s} \sum_{n=0}^{\infty} e^{j\nu(\phi+2\pi n)} H_\nu^{(1)}(K_0 r_>)\, H_\nu^{(1)}(K_0 r_<) \frac{H_\nu^{(2)}(K_0 a)}{H_\nu^{(1)}(K_0 a)} \times \frac{\left(-\log' H_\nu^{(2)}(K_0 a) + \log' H_\nu^{(2)}(K_1 a)\right)}{\frac{\partial}{\partial \nu}\left(\log' H_\nu^{(1)}(K_0 a) - N \log' H_\nu^{(2)}(K_1 a)\right)_{\nu=\nu_s}} \qquad \text{(A3.7.4)}$$

Employing the Wronskian(16) results in:

$$U(r,\phi) \sim -\frac{j}{K_0 a} \sum_{\nu_s} \sum_{n=0}^{\infty} \frac{e^{j\nu(\phi+2\pi n)} H_\nu^{(1)}(K_0 r_>)\, H_\nu^{(1)}(K_0 r_<)}{\left[H_\nu^{(1)}(K_0 a)\right]^2 \frac{\partial}{\partial \nu}\left(\log' H_\nu^{(1)}(K_0 a) - N \log' H_\nu^{(2)}(K_1 a)\right)} \qquad \text{(A3.7.5)}$$

Substituting the asymptotic forms and neglecting all terms $O\left[1/K_0 a\sqrt{N^2-1}\right]$:

$$U(r,\phi) \sim -\frac{j}{K_0 a} \sum_{\nu_s} \sum_{n=0}^{\infty} \frac{e^{jK_0\left(\sqrt{r_>^2-\left(\frac{\nu}{K_0}\right)^2} - \nu \cos^{-1}\frac{\nu}{K_1 r_>}\right) + jK_0\left(\sqrt{r_<^2-\left(\frac{\nu}{K_0}\right)^2} - \nu \cos^{-1}\frac{\nu}{K_0 r_<}\right)}}{\frac{\pi}{2}K_0\left[\sqrt{r_>^2-\left(\frac{\nu}{K_0}\right)^2}\sqrt{r_<^2-\left(\frac{\nu}{K_0}\right)^2}\right]^{1/2}\left[\frac{2}{\pi}\left(\frac{6}{K_0 a}\right)^{1/3} e^{-j\pi/3} A_i(g)\right]^2}$$

$$\times \frac{e^{-j\pi/2 + j\nu(\phi+2\pi n)}}{\frac{\partial}{\partial \nu} C_1\Big|_{\nu=\nu_s}} \qquad \text{(A3.7.6)}$$

Where:

$$\frac{\partial}{\partial \nu} C_1 = \frac{\partial}{\partial \nu}\left(\frac{H_\nu^{(1)'}(K_0 a)}{H_\nu^{(1)}(K_0 a)} - N \frac{H_\nu^{(2)'}(K_1 a)}{H_\nu^{(2)}(K_1 a)}\right)$$

$$= \frac{H_\nu^{(1)}(K_0 a)\frac{\partial}{\partial \nu} H_\nu^{(1)'}(K_0 a) - H_\nu^{(1)'}(K_0 a)\frac{\partial}{\partial \nu} H_\nu^{(1)}(K_0 a)}{H_\nu^{(1)}(K_0 a)}$$

$$- N \frac{\partial}{\partial \nu}\left(\frac{j}{K_0 a}\sqrt{(K_1 a)^2 - \nu^2}\right)$$

$$= \frac{\frac{2}{\pi} Y A(g) \frac{2}{\pi}\frac{Y^3}{3} g A(g) + \frac{2}{\pi} Y^2 A'(g) \frac{2}{\pi} Y^2 A'(g)}{\left[\frac{2}{\pi} Y \; A(g)\right]} + \frac{N j \nu}{K_1 a}\left((K_1 a)^2 - \nu^2\right)^{-1/2}$$

$$= \frac{Y^2 g}{3} + Y^2\left[\frac{A'(g)}{A(g)}\right]^2 + \frac{\nu j}{K_0 a}\left((K_1 a)^2 - \nu^2\right)^{-1/2}$$

$$= \frac{2}{K_0 a} e^{-j\pi}(\nu - K_0 a) - N^2\left[1 - \left(\frac{\nu}{K_1 a}\right)^2\right] + \frac{\nu j}{K_0 a \sqrt{(K_1 a)^2 - \nu^2}} \qquad \text{(A3.7.7)}$$

AT $\nu_s = K_0 a$

$$\frac{\partial}{\partial \nu} C_1\Big|_{\nu=\nu_s} = -N^2\left[1 - \left(\frac{1}{N}\right)^2\right] + \frac{j}{K_1 a\sqrt{1-N^2}}$$

$$\sim -(N^2 - 1) \qquad \text{(A3.7.8)}$$

$$U(r,\phi) \sim \sum_n \sum_{\nu_s} \frac{\frac{\pi}{2K_0}(K_0 a)^{-1/3} 6^{-2/3} e^{j\pi/6}\left[A(g)\right]^{-2}(N^2-1)^{-1} e^{jK_0\left(\sqrt{r_>^2 - a^2} + \sqrt{r_<^2 - a^2}\right)}}{\left(\sqrt{r_>^2 - a^2}\sqrt{r_<^2 - a^2}\right)^{1/2}} \qquad \text{(A3.7.9)}$$

$$\times e^{-jK_0 a\left(\cos^{-1}\frac{a}{r_>} + \cos^{-1}\frac{a}{r_<}\right) + jK_0 a(\phi + 2\pi n)}$$

LET $D_{11s}^2 = \sqrt{\frac{2\pi}{K_0}}\,\pi\, 6^{-2/3} e^{j5\pi/12}(K_0 a)^{-1/3}(N^2-1)^{-1}\left[A(g)\right]^{-2}$

AND $l_{1+} = 2\pi n + \phi - \cos^{-1}\frac{a}{r_<} - \cos^{-1}\frac{a}{r_>}$

$$\therefore U_r(r,\phi) \sim \sum_s \frac{A_0 D_{11s}^2 \, e^{jK_0(R + R_0) + j\nu_s/a \, l_1}}{(R R_0)^{1/2}} \qquad r \geq a \qquad 0 < |\phi| < 2\pi \qquad \text{(A3.7.10)}$$

APPENDIX (A3.8)

EVALUATION OF EQUATION (3.3.5) BY THE METHOD OF RESIDUES

Evaluate the following equation by the method of residues for m = 1:

$$U_m(r,\phi) \sim \frac{j}{8}\int_{-\infty}^{\infty} e^{j\nu(\phi+2\pi n)} T_{12} T_{21} R_{22}^{m-1} H_\nu^{(1)}(k_0 r_>) H_\nu^{(1)}(k_0 r_<) \frac{H_\nu^{(2)}(k_0 a)}{H_\nu^{(1)}(k_0 a)} \left(\frac{H_\nu^{(1)}(k_1 a)}{H_\nu^{(2)}(k_1 a)}\right)^m d\nu \qquad \text{(A3.8.1)}$$

Let m = 1, and consider $T_{12}\ T_{21}$. When the logarithmic derivation functions are substituted and multiplied, the term is written as the product of two Wronskians, thus:

$$U_1(r,\phi) \sim \frac{j}{8}\int e^{j\nu(\phi+2\pi n)} \left[\frac{-\frac{4j}{\pi k_0 a} \times -\frac{4j}{\pi k_1 a}}{\left(\frac{H_\nu^{(1)\prime}(k_0 a)}{H_\nu^{(1)}(k_0 a)} - N\frac{H_\nu^{(2)\prime}(k_1 a)}{H_\nu^{(2)}(k_1 a)}\right)^2}\right] \frac{H_\nu^{(1)}(k_0 r_>)\ H_\nu^{(1)}(k_0 r_<)}{\left[H_\nu^{(1)}(k_0 a)\right]^2\left[H_\nu^{(2)}(k_1 a)\right]^2} d\nu \qquad \text{(A3.8.2)}$$

This is a function of the form $F(z) = \frac{f'(z)}{g(z)^2}$ with second order poles at ν_s. The residue of F(z) is:

$$R_s = \frac{1}{\left[\frac{\partial}{\partial z} g(z)\right]}\left\{\frac{\partial}{\partial z} f(z) - \frac{f(z)\frac{\partial^2}{\partial z^2} g(z)}{\frac{\partial}{\partial z} g(z)}\right\}\Bigg|_{z=z_s} \qquad \text{(A3.8.3)}$$

Substituting the appropriate asymptotic forms of the Hankel function and neglecting all terms $0\left[1/K_0 a\sqrt{N^2-1}\right]$ there results,

$$\frac{\partial f(z)}{\partial z} = \frac{-2j\, e^{j(\phi+2\pi n)+j\left(\sqrt{(k_0 r_>)^2-\nu^2}-\nu\cos^{-1}\frac{\nu}{k_0 r_>}\right)-\frac{j\pi}{4}}}{\pi^2(k_0 a)(k_1 a)\ \pi/2\left(\sqrt{(k_0 r_>)^2-\nu^2}\right)^{1/2}\left(\sqrt{(k_0 r_<)^2-\nu^2}\right)^{1/2}}$$

$$\times \frac{e^{j\left(\sqrt{(k_0 r_<)^2-\nu^2}-\nu\cos^{-1}\frac{\nu}{k_0 r_<}\right)-j\pi/4+2j\left(\sqrt{(k_1 a)^2-\nu^2}-\nu\cos^{-1}\frac{\nu}{k_1 a}\right)-j\pi/2}}{\left[\frac{2}{\pi}\left(\frac{6}{k_0 a}\right)^{1/3} e^{-j\pi/3} A(q)\right]^2\left(\pi/2\ \sqrt{(k_1 a)^2-\nu^2}\right)^{-1}}$$

$$\times\left(\phi+2\pi n-\cos^{-1}\frac{\nu}{k_0 r_>}-\cos^{-1}\frac{\nu}{k_0 r_<}-2\cos^{-1}\frac{\nu}{k_1 a}\right) \qquad \text{(A3.8.4)}$$

From Appendix (A3.7)

$$\left[\frac{\partial}{\partial z} g(z)\right] = N^4 \left[1 - \left(\frac{\nu}{K_1 a}\right)^2\right]^2$$

The value of the second term of (A3.8.3) is found to be of higher order, and is neglected.

Thus,

$$U_i(r,\phi) \sim 2\pi j \sum_{\nu_s} \frac{\left[N^2 - \left(\frac{\nu}{K_0 a}\right)^2\right]^{3/2}}{2 K_0 a} \frac{\left(\phi + 2\pi n - \cos^{-1}\frac{\nu}{K_0 r_7} - \cos^{-1}\frac{\nu}{K_0 r_2} - 2\cos^{-1}\frac{\nu}{K_1 a}\right)\left(\frac{6}{K_0 a}\right)^{2/3} e^{j\frac{2\pi}{3}}}{(R R_0)^{1/2}}$$

$$\times \left[A(g)\right]^{-2} e^{j k_0 (R + R_0) + 2 j K_1 a \cos\theta_c + j \nu_s \omega_{21} - j\pi/2} \qquad \text{(A3.8.5)}$$

LET $\quad D_{12} = (N^2 - 1)^{-1/2} \qquad D_{21} = 2 \qquad$ AND

$$\omega_{2+} = \phi + 2\pi n - \cos^{-1}\frac{a}{r_7} - \cos^{-1}\frac{a}{r_2} - 2\cos^{-1}\theta_c$$

Then,

$$U_r(r,\phi) \sim \sum_s A_0 D_{11s}^2 D_{12} D_{21} (R R_0)^{-1/2} \omega_{2+} e^{j K_0 (R + R_0) + j K_1 a \cos\theta_c + j \nu_s \omega_{2+} - j\pi/2} \qquad \text{(A3.8.6)}$$

which is given in Equation (3.3.10).

APPENDIX (A4.1)

SAMPLE CALCULATION

From Fig. (4.1.1), the field is determined at the point Ky = 15.

(A) The incident field at P is:

$$U_i \sim \frac{A_o}{\sqrt{R_i}} e^{jK_oR_i}$$

where $R_i = \sqrt{(605)^2 + (2.98)^2} \sim 605$ cm

Let the phase reference be $\gamma_o = K_o\ 605 = o$

where $K_o = 5.03.$

$$\therefore \qquad U_i \sim \frac{A_o}{24.6} e^{jo} .$$

(B) The reflected field at P is:

$$U_r \sim A_o R_{11} (R_r)^{-1/2} (1 + \frac{Q_r}{C_r})^{-1/2} e^{jK_o(R_r+Q_r-R_i)}$$

From Fig. (A4.1.1) $\theta_i = 81^o$, determined by construction.

Thus $$R_{11} = \frac{\cos\theta_i - N\cos\theta_r}{\cos\theta_i + N\cos\theta_r} = -.780$$

By measurement, $Q_r = 5.50$ cm , $R_r = 599.78$ cm

$$\frac{1}{C_r} = \frac{2}{a\cos\theta_i} = 11.1$$

$$\sqrt{1 + \frac{Q_r}{C_r}} = 7.878$$

and

$$U_r \sim -\frac{A_o}{248} e^{j\ 81^o}$$

When compared to the incident field,

$$\frac{U_r}{U_i} \sim .0992\ e^{j-99^o}$$

(C) The field at P due to the first transmitted ray is:

$$U_1 \sim \frac{A_o\, T_{12}\, T_{21}\, e^{j K_o(R_1+Q_1-R_i) + j K_1 L_1}}{\sqrt{R_1}\,\sqrt{1 + \frac{Q_1}{C_1}}\,\sqrt{1 - \frac{L_1}{b_1}}}$$

From Fig. (A4.1.1), $\theta_i = 46.5^o$, $R_1 = 599.13$ cm

$Q_1 = 4.89$ cm, and $L = 2.275$ cm.

Thus $R_{11} = -.3492$, $T_{12} = 0.651$, $T_{21} = 1.349$

$$\frac{1}{b_1} = \frac{1}{a \cos \theta_r}\left[1 - \frac{\cos \theta_i}{N \cos \theta_r} - \frac{a \cos^2 \theta_i}{R_1\, N \cos \theta_r}\right]$$

$$= .457$$

$$\frac{1}{C_1} = \frac{\cos \theta_r}{\cos \theta_i}\left[\frac{N \cos \theta_r}{L-b_1 \cos \theta_i} - \frac{N}{a \cos \theta_i} + \frac{1}{a \cos \theta_r}\right]$$

$$= 35.5$$

$$\sqrt{1 - \frac{L}{b_1}} = j\ 0.197$$

$$\sqrt{1 + \frac{Q_1}{C_1}} = 13.2$$

$$\therefore \quad U_1 \sim \frac{A_o}{72.4\, j}\, e^{j\, 46^o} \sim \frac{A_o}{72.4}\, e^{j -44^o}$$

When compared to the incident field,

$$\frac{U_1}{U_i} \sim 0.34^o\, e^{j-44^o}$$

(D) The field at P due to the third transmitted ray is:

$$U_3 \sim \frac{A_o\, T_{12} T_{21}\, R_{22}^{\,2}\, e^{jK_o(R_3+Q_3-R_i) + j K_1\, 3L}}{\sqrt{R_3}\,\sqrt{1+Q_3/C_3}\,\sqrt{1-L/b_1}\,\sqrt{1-L/b_2}\,\sqrt{1-L/b_3}}$$

From Fig. (A2.1.2), $\theta_i = 15.9^o$, $R_3 = 598.77$ cm.

$Q_3 = 4.59$ cm, $L = 2.50$ cm.

$R_{11} = -0.242$, $R_{22} = .242$, $R_{22}^2 = .0586$

$T_{12} = 0.758$, $T_{21} = 1.242$.

$$\sqrt{1 + Q_3/C_3} = \sqrt{1 + 4.59 \times 5.14} = 1.833$$

$$\sqrt{1 - L/b_3} = \sqrt{1 - 2.50 \times 1.137} = i\ 1.357$$

$$\sqrt{1 - L/b_2} = \sqrt{1 - 2.50 \times 2.987} = i\ 2.544$$

$$\sqrt{1 - L/b_1} = \sqrt{1 - 2.50 \times 0.311} = 0.4712$$

$$U_3 \sim \frac{A_o}{1345\ j^2}\ e^{j\ 100^o} \sim \frac{A_o}{1345}\ e^{j-80^o}$$

When compared to the incident field

$$\frac{U_3}{U_i} \sim .018\ e^{j-80^o}$$

The total field as a ratio of the incident field is:

$$\begin{aligned}\frac{U(P)}{U_i(P)} &= 1 + .0992\ e^{j-99^o} + .340\ e^{j-44^o} + .018\ e^{j-80^o} \\ &= 1.27\ e^{j-21^o}\ .\end{aligned}$$

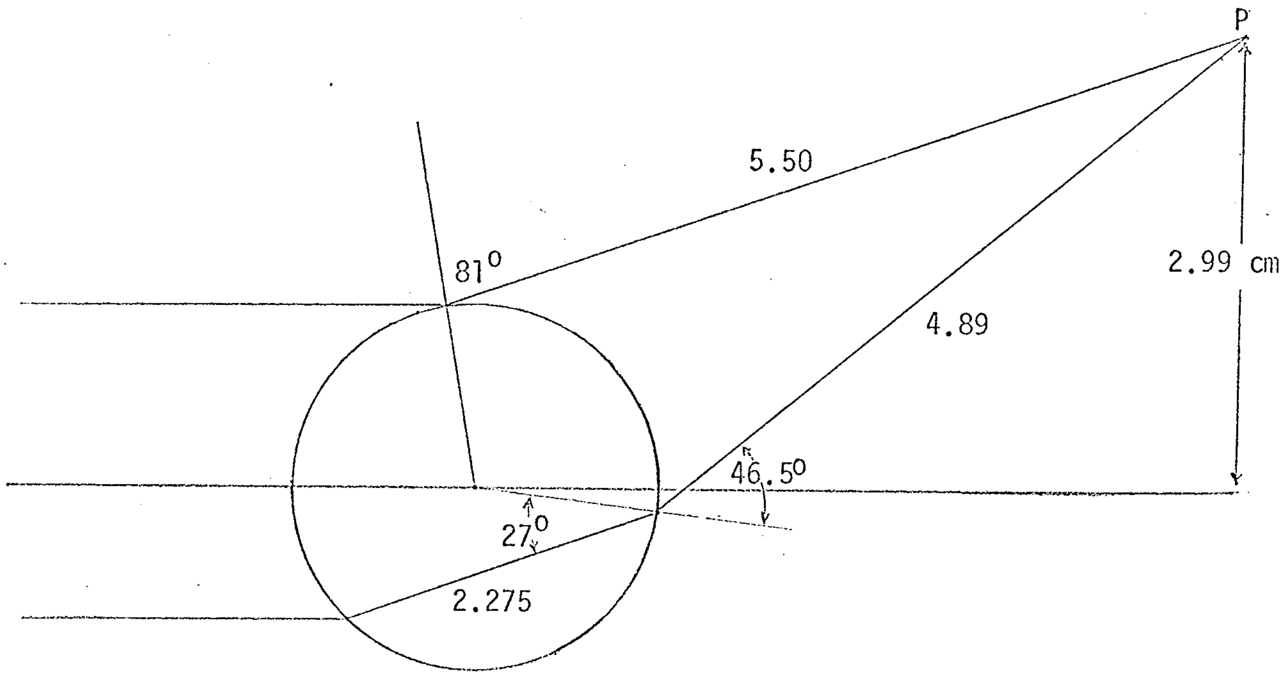

FIGURE (A4.1.1)

REFLECTED AND FIRST TRANSMITTED RAY, Ky = 15

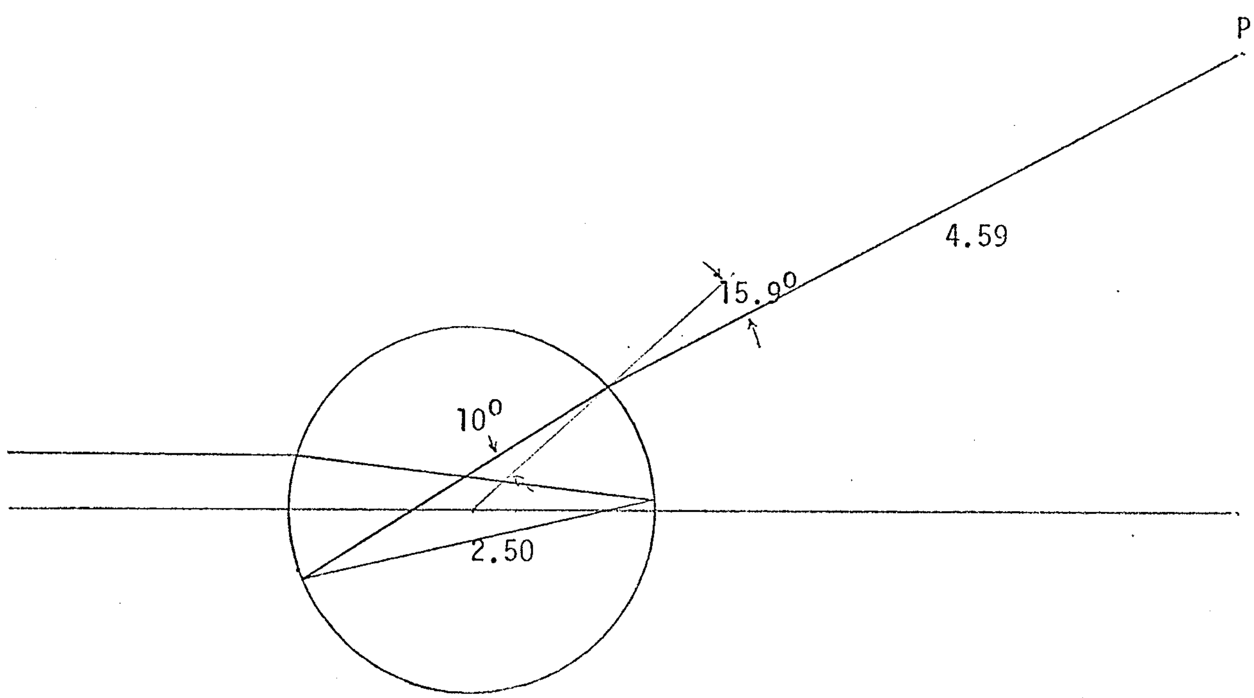

FIGURE (A4.1.2)

THIRD TRANSMITTED RAY

REFERENCES

(1) Keller, J.B., "A Geometrical Theory of Diffraction" Proceeding of the Symposium in Applied Mathematics, McGraw Hill. Vol.8, 1958, pp. 27-52.

(2) Keller, J.B., "Geometrical Theory of Diffraction", Journal of the Optical Society of America, Vo. 52, No. 2, February 1962. pp. 116-130.

(3) Collin, R.E., "Field Theory of Guided Waves", McGraw Hill, 1960.

(4) Stratton, J.A., "Electromagnetic Theory", McGraw-Hill, 1941, Chap. 9, Sec. 10.

(5) Keller, J.B., "Diffraction by a Convex Cylinder", IRE, Transactions on Antennas and Propagation, Vol.4, No.3, July 1956, pp. 312.

(6) Levy, B.R., Keller, J.B., "Diffraction by a Smooth Object", Communications on Pure and Applied Mathematics, Vol. 12, 1959, pp. 159

(7) Keller, J.B., "Diffraction by an Aperture", Journal of Applied Physics, Vol. 28, 1957, pp. 426-444.

(8) Burke, J.E., and Keller, J.B., "Diffraction of Finite Bodies of Revolution", Sylvania Electronics Systems Engineering Report No. EDL-E49, April 1960.

(9) Konyoumjian, R.G., Peters, L., Thomas, D.T., "A Modified Geometrical Optics Method for Scattering by Dielectric Bodies", IEE Transactions on Antennas and Propagation. November 1963.

(10) Kay, I., Keller, J.B., "Asymptotic Evaluation of the Field at a Caustic", Journal of Applied Physics, Vol. 25, No. 7, July 1954, pp. 876-883.

(11) Smirnov, U.I., "A Course of Higher Mathematics", Vol. III, Part II, Pergamon Press, 1964.

(12) Streifer, W., Kodis, R.D., "On the Scattering of Electromagnetic Waves by a Dielectric Cylinder", Quarterly of Applied Mathematics, Vol. 22, No. 3, (1964), pp. 193.

(13) Goertzel, G., Tralli, N., "Some Mathematical Methods of Physics", McGraw Hill, 1960, pp. 181.

(14) Rubinow, S.I., "Scattering from a Penetrable Sphere at Short Wavelengths", Annals of Physics, Vol. 14, 1961, pp. 305-332.

(15) Ambramowitz, M., Stegun, I.A., "Handbook of Mathematical Functions", U.S. Dept. of Commerce, 1964.

(16) Franz, W., Beckmann, P., "Creeping Waves for Objects of Finite Conductivity", IRE Transactions on Antennas and Propagation, Vol.4, No. 3, July 1956, pp. 203.

(17) Froese, C., Wait, J.R., "Calculated Diffraction Patterns of Dielectric Rods at Centimeter Wavelengths", Canadian Journal of Physics, Vol. 32, 1954, pp. 775.

(18) Kodis, R.D., "Diffraction Measurements at 1.25 Centimeters", Journal of Applied Physics, Vol. 23, No. 2, Feb. 1952, pp. 249.

(19) Lord Rayleigh, "On the Electromagnetic Theory of Light", Philosophical Magazine, Vol. 12, Aug. 1881, pp. 379.

(20) Sommerfield, A.J.W., "Partial Differential Equations in Physics", Academic Press Inc., 1949.

(21) VandeHulst, H.C., "Light Scattering by Small Particles", J. Wiley & Sons, Inc., 1957.

(22) Lebedev, N.N., "Special Functions and Their Applications", Prentice-Hall, Inc., 1965.

(23) Morse, P.M., Feshback, H., "Methods of Theoretical Physics", McGraw-Hill, 1953.

(24) Harrington, R.F., "Time-Harmonic Electromagnetic Fields", McGraw-Hill, 1961.

(25) McLachlan, N.W., "Bessel Functions for Engineers", Oxford University Press, 1934.

(26) Watson, G.N., "A Treatise on the Theory of Bessel Functions", Cambridge University Press, 1944.

(27) Whittaker, E.T., and Watson, G.N., "A Course of Modern Analysis", Cambridge University Press, 1927.